Met Monograph No.:
MoES/IMD/SAT. MET./GNSS/01(2022)/11

Government of India
Ministry of Earth Sciences
India Meteorological Department

Meteorological Applications of Indian GNSS derived IPWV

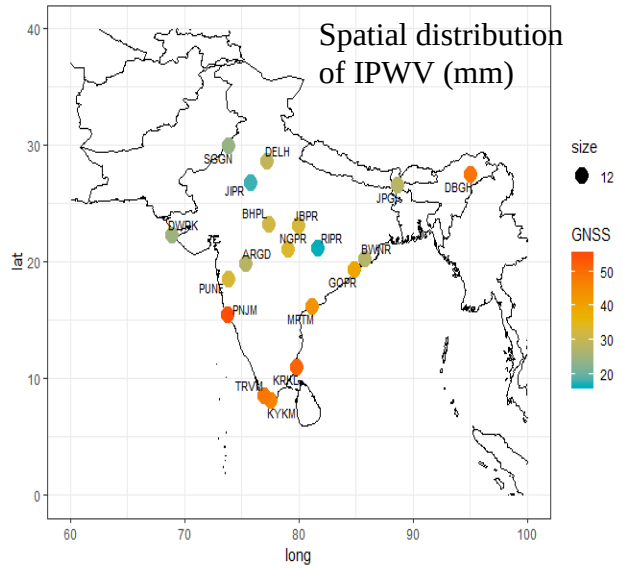

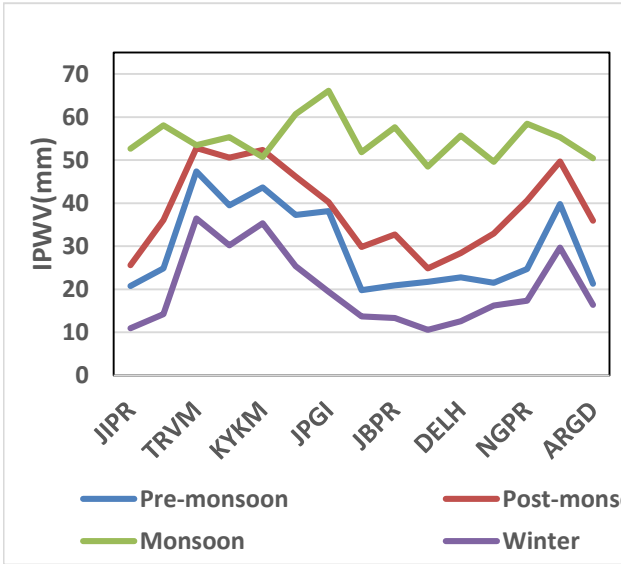

Seasonal Variations of IPWV (mm).

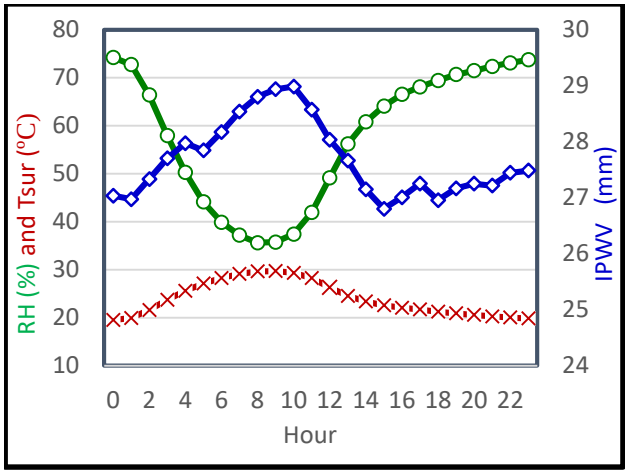

Diurnal Variations of IPWV (mm), Surface temperature (T_{sur} °C) and Relative Humidity (RH %) over Delhi.

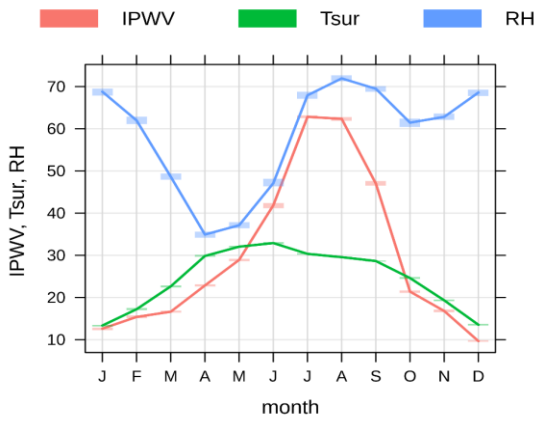

Monthly Variations of IPWV (mm), Surface temperature (°C) and Relative Humidity (%) over Delhi.

Ramashray Yadav, R.K. Giri, N. Puviarasan and S.C. Bhan
Satellite Meteorology Division
India Meteorological Department, Lodi Road, New Delhi
2022

Met Monograph No.:
MoES/IMD/SAT. MET./GNSS/01(2022)/11

Meteorological Applications of Indian GNSS derived IPWV

Ramashray Yadav, R.K. Giri, N. Puviarasan and S.C. Bhan

INDIA METEOROLOGICAL DEPARTMENT
Ministry of Earth Sciences
Government of India
New Delhi

2022

Copyright
© 2022 by India Meteorological Department
All Rights Reserved.

Disclaimer and Limitations

IMD is not responsible for any errors and omissions.

Published in India

By

Satellite Meteorology Division, India Meteorological Department,
Lodi Road, New Delhi, Pin: 110003
Ph. : 011 – 43824535, Email: ramashray.5329@gmail.com

PREFACE

Total precipitable water is a key variable needed for operational weather forecasting. India Meteorological Department (IMD) started Global Navigation Satellite System (GNSS) Pilot Phase project for measuring the total Integrated Precipitable Water Vapour (IPWV) in 2005 over the 5 stations (New Delhi, Guwahati, Kolkata, Mumbai, and Chennai). The Network was further extended with additional 25 stations covering most of the important areas which are responsible for weather monitoring. Near real-time GNSS data of high temporal resolution and accuracy helps in many atmospheric activities like the onset, progress and withdrawal of the monsoon; and monitoring & nowcast of thunderstorms, cyclone, fog, heavy rainfall events, etc. Utilization of GNSS data in many other activities like IPWV thresholds for initiation of rainfall/thundershower for each station, annual, seasonal, monthly, and diurnal variations of IPWV are also included in this report which could act as important guidelines for the forecasters and other stakeholders.

I extend my compliments to Shri Ramashray Yadav, Dr. R.K. Giri, N. Puviarasan and Shri S.C. Bhan for bringing out this important publication.

January 2022
New Delhi

Dr. Mrutyunjay Mohapatra
Director General of Meteorology

CONTENTS

S.No.	Description	Page
1	Introduction	7-9
2	GNSS Meteorology	10-15
3	Climatology	16-32
	3.1 Annual Variations of IPWV	16-17
	3.2 Seasonal and Monthly variations of IPWV	18-23
	3.3 Diurnal variation of IPWV	29-32
4	Validation	33-44
	4.1 Validation of GNSS IPWV with GPS sonde IPWV	33-38
	4.2 Inter-comparison of GNSS- IPWV with INSAT-3D IPWV	39-40
	4.3 Inter-comparison of GNSS- IPWV with INSAT-3DR sounder and CAMS reanalysis data	40-44
5	Month wise IPWV threshold generation for each GNSS station	45-48
6	Preliminary Analysis of the relationship between GNSS-IPWV and Rainfall: Case studies	49-52

INDIA METEOROLOGICAL DEPARTMENT

Document & Data Control Sheet

1	**Document title**	Meteorological Applications of Indian GNSS derived IPWV
2	**Document type**	Met Monograph
3	**Issue No.**	MoES/IMD/SAT. MET./GNSS/01(2022)/11
4	**Issue date**	2022
5	**Security Classification**	Unclassified
6	**Control Status**	Uncontrolled
7	**No. of Pages**	58
8	**No. figures**	15
9	**No. of reference**	50
10	**Distribution**	Unrestricted
11	**Language**	English
12	**Authors**	Ramashray Yadav, R.K. Giri, N. Puviarasan and S.C. Bhan
13	**Originating Division/Group**	Satellite Meteorology Division
14	**Reviewing authority**	Dr. V.K. Soni
15	**Approving Authority**	DGM
16	**End users**	Ministries / Departments of Central and State Governments, World Environmental community, Research organizations, Scientific community, Planners, Public etc.
17	**Abstract**	Ground based Global Navigational Satellite System (GNSS) receivers for continuous monitoring of tropospheric total integrated precipitable water vapour (IPWV) and its continuous observation along with pressure, temperature and humidity data is a useful tool for nowcasting, monsoon studies, thunderstorms observation, dust storms and climate research. This report brings out the variations in the behavior of IPWV estimated from IMD ground-based GNSS network over the Indian region located at coastal, inland and desert stations in terms of diurnal, monthly, seasonal, and annual variations for the period 2017-2020. Monthly IPWV thresholds for initiation of rainfall have been generated for all the stations to utilize these thresholds in now-casting as well as forecasting the weather events.
18	**Key words**	Integrated Precipitable Water Vapur, IMD, GNSS, Monsoon.

Chapter-1
Introduction

India Meteorological Department (IMD) is the nodal agency of the Government of India for deploying weather instruments, collection of meteorological data, utilization in daily operational work of weather forecasting and to provide all weather-related services to the people of this country and neighbourhood and sharing of data with various research institutes all over the world. Improving the quality of operational services is one of the main and important objectives of the Meteorological Department. The Department is constantly implementing and upgrading the observational technology and inducting new technology to the maximum possible extent as and when required to meet this requirement.

The 'Global Navigation Satellite System' (GNSS) refers to a constellation of satellites providing signals from space transmitting positioning and timing data. By definition, a GNSS provides signals on global coverage for example GPS (Global Positioning System - USA), GLONASS (Global Navigational Satellite System -Russia), Galileo (Europe), and CNSS (Compass/BeiDou Navigation Satellite System) / BDS (BeiDou Navigation System) (China), IRNSS/NAVIC (Indian Regional Navigation Satellite System – India) and QZSS (Quasi-Zenith Satellite System - JAPAN) are some of the important global or regional Navigational Satellite Systems. Precise location information of interest to geophysicists required correction of position errors due to atmospheric delays. In the early 1990's, scientists developed techniques to use these atmospheric delay errors as signals to determine the amount of total water vapour content in the troposphere, popularly known as Integrated Precipitable Water Vapor (IPWV). These efforts created a new science, GPS/GNSS Meteorology.

IMD has installed a network of 25 ground-based GNSS (Global Navigational Satellite System) receivers with co-located Meteorological sensor at 25 number locations (Fig. 1) for continuous monitoring of troposphere total IPWV every 15 min interval or less with the primary purpose of assimilation of IPWV data into the Numerical Weather Prediction models and to act as an additional tool for nowcasting of thunderstorms, dust storms, monsoon studies and for climate research. A variety of techniques exist for measuring the atmospheric IPWV, which can be divided into different categories such as in situ measurements, satellite-based measurements, and model-based reanalysis. In-situ GPS-based Radiosonde observations generally suffer from poor

spatiotemporal resolutions;. Yadav et al. (2020) carried out the validation of PWV estimated from Indian GNSS networks with GPS Sonde data for the period of June 2017 to May 2018 over the Indian region and found reasonably well agreement with GPS sonde observations over different geographical locations of Indian regions. He reported a positive bias of less than 4.0 mm, a correlation coefficient > 0.85, and RMSE <5.0 mm. Turner et al. (2003) reported a 5 % dry bias with Microwave Radiometer. Miloshevich et al., 2009, found a similar limitation of Relative Humidity measurement with Vaisala RS92 Radiosonde and developed an empirical correction to remove the mean bias error. The principle of differential optical absorption spectroscopy in the red spectral range was used to retrieve the IPWV in both the Global Ozone Monitoring Experiment (GOME) and Scanning Imaging Absorption Spectrometer for Atmospheric CHartography (SCIAMACHY) by Beirle et al. (2018). Atmospheric Infrared Sounder (AIRS) is a hyperspectral instrument that collects radiances in 2378 IR channels with wavelengths ranging from 3.7 to 15.4 µm. Aumann et al. (2003) utilized clear sky radiances of AIRS in the retrieval of column integrated water vapour which is contributed by some channels having different sensitivity towards water vapour content present in the atmosphere. Moderate Resolution Imaging Spectroradiometer (MODIS) utilizes an infrared algorithm that employs ratios of water vapor absorbing channels centered near 0.905 µm, 0.936 µm, and 0.940 µm with atmospheric window channels at 0.865 µm and 1.24 µm for estimating the precipitable water vapour (Kaufman and Gao, 1992). The ratios partially remove the effects of variation of surface reflectance with wavelengths and result in the atmospheric water vapor transmittances. The column water vapor amounts are derived from the transmittances based on theoretical calculations and using lookup table procedures. At present two advanced Indian geostationary meteorological satellites INSAT-3D (launched on 26th July 2013) and INSAT-3DR (launched on 6th September 2016) with similar sensor characteristics are orbiting over the Indian region. These satellites placed at 82° East and 74° east longitude in the geostationary orbit are equipped with 19 channels infrared sounders used to retrieve meteorological parameters like the profiles of temperature, humidity, and ozone, atmospheric stability indices, layer, total precipitable water vapor, etc. at 1 hour (sector A- Indian landmass region) and 1.5 hours (sector B-Indian ocean region) intervals (Kishtawal et al., 2019). Temperature and humidity (T-q profile) is used to retrieve thermodynamic indices which is useful in analyzing the strength and severity of severe weather events. Retrievals from reanalysis data set Modern-Era Retrospective Analysis for Research and Applications-2 (MERRA-2) (Gelaro et al., 2017) and Climate Forecast System Reanalysis (CFSR) Data Archive (https://rda.ucar.edu/pub/cfsr.html) utilized 3d-var data assimilation techniques and reasonably

reproduce the characteristics of climatology, annual cycle and the interannual variations of precipitable water vapour in the south of Central Asia (Saha et al., 2010; Jiang et al., 2019). The study carried out by Berrisford et al. (2011) found that ERA-interim data set is superior in quality to ERA-40 during the period 1989-2008.

In the past few decades, GNSS-derived IPWV has been widely used in meteorological applications such as in numerical models, climate studies, and weather forecasting (Bevis et al., 1992, 1994; Koulali et al., 2012; Rohm et al., 2014; Emmanuel et al., 2018). Many researchers in the past have been studied and reported diurnal variation of integrated precipitable water vapor over different parts of the globe (Wang et al., 2007; Kimura et al., 1997; Güldner and Spänkuchetal., 1999; Kuwagata et. al., 2001; Ohtani et al., 2001; Bouma et al., 2002; Wu et al., 2003; Pramualsakdikul et al., 2007; Ortiz de Galisteo et al., 2011). The IPWV diurnal cycle over Europe is strongest in the summer season, weaker in winter, and negligible in the spring season having spatial variability of IPWV over different parts of Spain. Diurnal variations in precipitation and convection have been observed by many researchers (Haldar et al. 1991; Liu et al. 2009; Murakami et al., 1983; Nitta and Sekine**.,** 1994; Oki and Musiake., 1994; Dai et al., 2001, 2002; Ohsawa et al., 2001, Stevens et al., 2017). Significant regional variability of IPWV has been reprted in global analyses of IPWV data (Chen et al., 2016; Parracho et al., 2018; Mieruch et al., 2008; Trenberth et al., 2003) and there is a need to carry out regional studies to investigate how representative these global changes are. Emmanuel et al. (2018) have reported IPWV maximum around midnight over Trivandrum and late evening over Gadanki. They also reported that diurnal variation in IPWV is mainly controlled by the local circulation. Puviarasan et al. (2015) found that variation in the tropospheric precipitable water content is another indicator of the state of the monsoon onset and reported that there is increase in precipitable water (PW) content during the arrival of monsoon and there is a decrease in PW during monsoon retreat.

This study brings out the behavior of IPWV estimated from IMD ground-based GNSS stations over the Indian region located at Inland, coastal and desert places in terms of diurnal, monthly, seasonal, and annual variations in the Indian region for the period 2017-2020. Monthly IPWV thresholds have been generated from 4 years of IMD GNSS data for all the stations to utilize further these thresholds in now-casting as well as forecasting the weather events.

Fig. 1. India Meteorological Department Global Navigation Satellite System (GNSS) receiver network

Chapter-2

GNSS Meteorology

In GNSS positioning, the fundamental observable of GNSS is the signal propagation time from a satellite to a receiver. Multiplying the propagation time by the speed of light in a vacuum gives the pseudo-range between the satellite and the receiver. The pseudo-range is a mix of various errors like clock errors (both on receiver and satellite), atmospheric error, multipath error, etc. For geodetic applications, higher accuracies (millimeter level), carrier phase measurements are necessary because the phase can be measured to 1 % of the wavelength of the carrier signal.

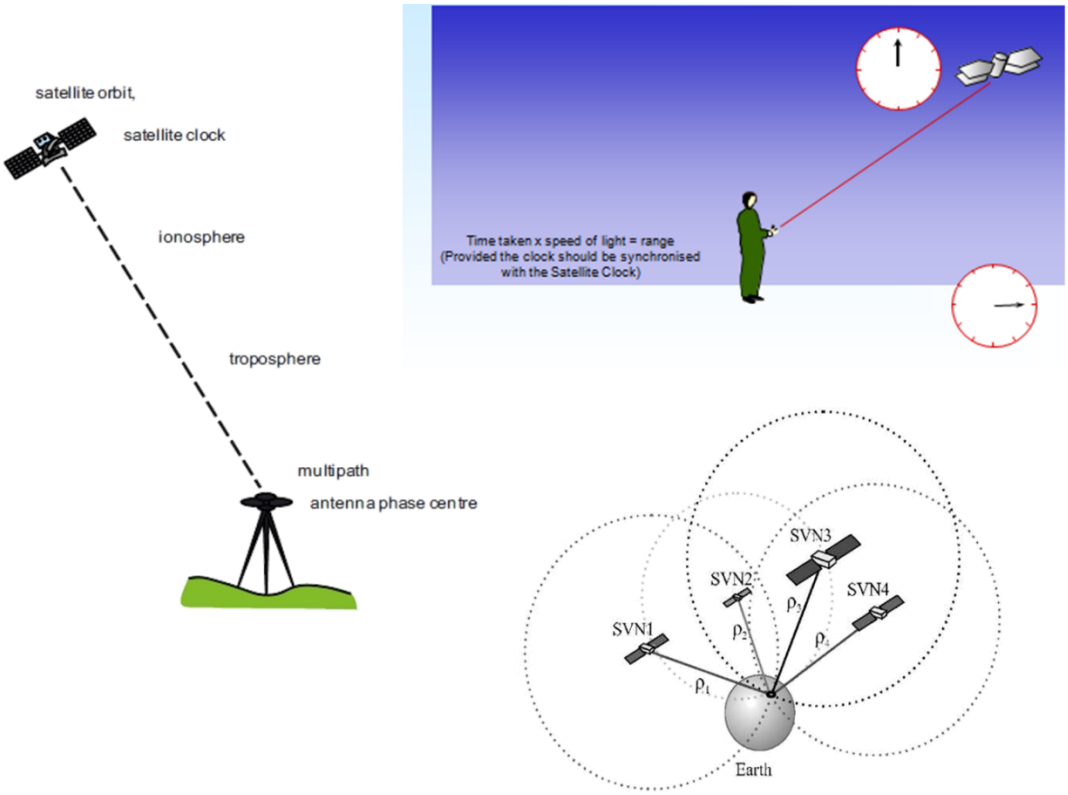

Fig. 2. User Segments and User finding his range from the GNSS satellite.

As depicted in Fig. 2**,** the total GPS signal delay (error) in the atmosphere is composed of ionospheric and tropospheric delays. The largest atmospheric signal delays come from the ionosphere. These delays can be compensated with dual-frequency GPS receivers. GPS satellites send radio signals at two frequencies, L1 (1.6 GHz) and L2 (1.2 GHz). The delay in the ionosphere is inversely proportional to the frequency of the radio waves. Thus, the delay can be calculated by measuring the difference between the two frequencies. The tropospheric delay cannot be corrected by using the dual frequencies since the electrically neutral atmosphere (troposphere) is non dispersive below 30 GHz (Fig. 2). The tropospheric delay has two components: hydrostatic and

wet components (Fig. 3). The dry delay is due to the total mass of the atmosphere above the GPS antenna, and the wet delay is caused by the total amount of water vapor along the GPS signal path.

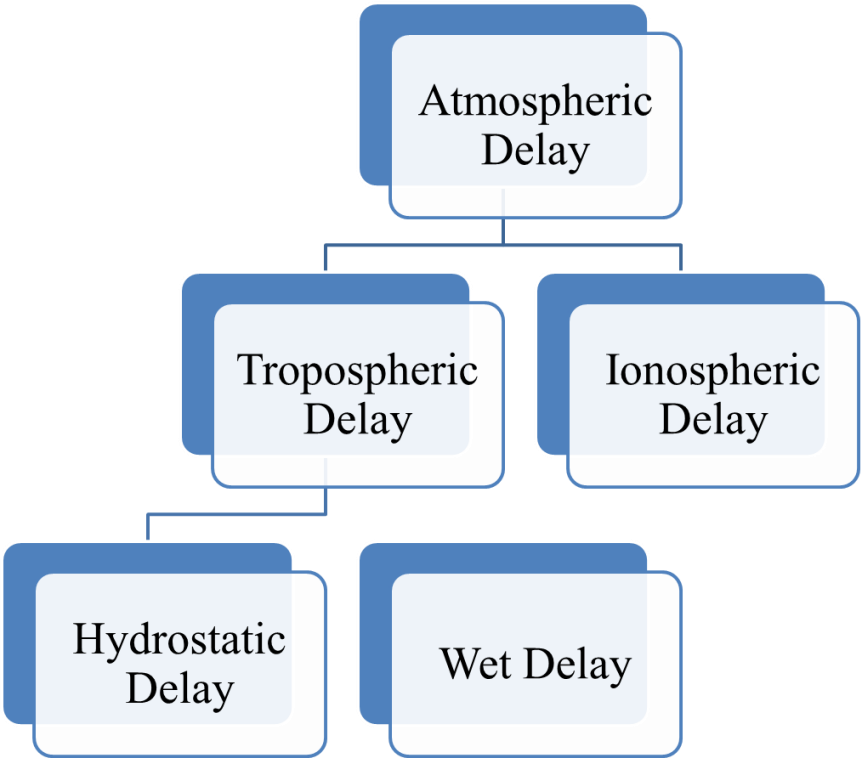

Fig. 3 GNSS Signal Delay

A carrier phase measurement in units of length can be expressed as follows-

$$\phi = D + c(T_r - T_s) - \Delta I + \Delta L + n\lambda + \varepsilon \quad \text{------ (1)}$$

where φ is the carrier phase observable and D is the true distance between the satellite and the receiver; c is the speed of light in vacuum; T_r and T_s are the receiver and satellite clock offsets which can be eliminated by double-difference techniques. ΔI, the ionospheric delay (phase advance) is frequency dependence can be estimated and removed by forming an ionospheric free linear combination using two carrier phase measurements at two different frequencies.

$$\left[R_{L1} - \frac{f^2_{L1}}{f^2_{L2}}\right]\frac{f^2_{L1}}{f^2_{L1} - f^2_{L2}} = D + c(T_r - T_s) \quad \text{-------} (2)$$

Where

$$R_{L1} = D + c(T_r - T_s) - \Delta I(f_{L1})$$
$$R_{L2} = D + c(T_r - T_s) - \Delta I(f_{L2})$$

From equation (2) 99.9% of ionospheric delay is calculated accurately and can be eliminated. *ΔL* is the total delay in the neutral atmosphere given by

$$\Delta L = 10^{-6}\int N(s)ds \quad \text{----------} (3)$$

ΔL is the sum of zenith hydrostatic delay and zenith wet delay given by (Bevis et al., 1992; Bevis et al., 1994; Davis et al., 2009)

$$\Delta L = \Delta L_h^0 + \Delta L_w^0 \quad \text{----------} (4)$$

The zenith hydrostatic delay (ZHD) can be estimated and eliminated by measuring surface pressure P_s

$$\Delta L_h^0 = ZHD = (2.2779 \pm 0.0024)\, p_s \,/\, f(\phi, H) \quad \text{-------} (5)$$

with ZHD in mm and P_s in hPa. The term

$$f(\phi, H) = 1.00266\cos 2\phi - 0.00028H \quad \text{------} (6)$$

accounts for the variation in gravitational acceleration with latitude φ and the height *H* of the surface above the ellipsoid (in kilometers). The ZWD is obtained by subtracting the ZHD from ZTD, the IPWV (mm) estimates were then derived by scaling the ZWD with the multiplication factor Π given by

$$PW = \Pi * ZWD \quad \text{----------} \ (7)$$

$$\Pi^{-1} = 10^{-6} \rho R_v [(k_3 / T_m) + k_2^{'}] \quad \text{-------} \ (8)$$

where ρ is the density of liquid water, R_v is the specific gas constant for water vapour, k_3, *and* $k_2^{'}$ are physical constants. The water-vapour weighted mean temperature T_m of the atmosphere is defined and approximated as (Wang et al, 2005)

$$Tm \equiv \frac{\int \frac{Pv}{T} dz}{\int \frac{Pv}{T^2} dz}$$

which can be obtained from RS/RW or NWP analysis. Assuming a linear relation with surface temperature it is also possible to approximate T_m from station surface temperature T_s. T_s and P_s are obtained at the GNSS site location using an installed meteorological sensor.

$$\mathbf{T_m = 55.8 + 0.77T_S}$$

Error due to T_m: Water vapour weighted vertically averaged mean temperature of the atmosphere T_m is an important parameter of the relationship between total precipitable water and the zenith wet delay because the accuracy of GPS estimates of precipitable water is directly related to the accuracy of T_m. The water-vapour weighted mean temperature of the atmosphere is defined and approximated as

$$Tm \equiv \frac{\int \frac{P_v}{T} dz}{\int \frac{P_v}{T^2} dz} \approx \frac{\sum_{i=1}^{N} \frac{P_{vi}}{T_i} \Delta Z_i}{\sum_{i=1}^{N} \frac{P_{vi}}{T_i^2} \Delta Z_i}$$

T_m is a function of the vertical profile of atmospheric temperature and humidity. Using equations, the relative error of PW due to errors in T_m is given by

$$\frac{\Delta PW}{PW} = \frac{\Delta \Pi}{\Pi} = \frac{1}{1 + \frac{k_2^{'}}{k_3} T_m} * \frac{\Delta T_m}{T_m}$$

Since $\frac{k_2^{'}}{k_3}$ is small (~5.9 x 10^{-5}). Hence the relative error of IPWV approximately equals to that of T_m. Based on the above equation for T_m values 240 K to 300 K, the 1% and 2% accuracies in IPWV require errors in T_m less than 2.74K and 5.48 K on average respectively [Wang et al.2005,]. Atmospheric temperature and humidity profiles, such as those from soundings, can be used to calculate Tm. A commonly used method for estimating Tm is to use the strong relationship between Tm and Ts (surface air temperature) since Ts can be obtained from either surface observations. However, the application of the Tm-Ts relationship is hampered because the relationship varies with space, time and weather conditions. The most commonly used Tm-Ts relationship is from Bevis et al. [1992], which was derived from radiosonde data at 13 U.S. sites over a 2-year period and gives a RMS error of ~4.74 K.

Table-1: Estimated Tm derived from different regression equations and from RSRW data for the three events over Delhi (Puviarasan et al., 2020)

Date/Time (UTC)		T_m (°K) (Nearest RSRW)	T_m from Surface Temperature (°K)					RSRW PW (mm)	GPS PW (mm)
			Bevis	Mendes	Solbrig	Schueler	IMD		
1st Aug 2007	0000	287.99	286.92	287.89	286.47	281.64	287.57	55.14	56.82
	1200	286.43	286.84	287.81	286.39	281.58	287.49	65.26	63.60
27th Jul 2009	0000	289.30	288.36	289.47	288.01	282.94	289.11	70.06	62.25
	1200	292.99	292.97	294.52	292.94	287.08	294.02	69.07	62.91

21st Aug 2009	0000	291.84	284.76	285.52	284.16	279.71	285.26	45.23	45.40
	1200	285.46	286.20	287.10	285.70	281.00	286.80	57.66	45.50

The uncertainty in Tm of 5 K corresponds to 1.7 – 2.0 % in PW (Hagemann et al., 2003).

Mapping functions: In GNSS data processing, the slant path delay is converted to the equivalent ZTD (sum of the ZHD and the ZWD) using hydrostatic and wet Mapping Functions (MFs) (Niell, 1996):

$$\Delta L = m_h(\theta)\Delta L_h^z + m_w(\theta)\Delta L_w^z$$

Where θ is the elevation angle seen from the ground antenna to the satellite.

The remaining term $n\lambda$ and ε in equation (1) is integer ambiguity and the sum of other unmodelled errors, e.g. signal multipath, antenna phase center variations, and radome effects can be estimated and removed from the long term observations.

Chapter-3
GNSS Climatology

3.1 Annual Variations of GNSS-IPWV

Analysis of the annual range of IPWV helps understand the local and temporal behavior of IPWV at a station. Owing to vast geographical variations across the country, the distribution of IPWV throughout the Indian region showed clear geographical differences. Distribution of IPWV using INSAT-3DR and CAMS reanalysis data over the Indian subcontinent shows the annual mean IPWV in the range of 0–50 mm over different regions of the country. A larger mean IPWVs values was observed over the coastal regions and high rainfall regions of northeast India as compared to inland and desert regions. The largest IPWV variation with a value of standard deviation (SD) ~16 mm was found over foothills of the Himalayas (Yadav et. al., 2021).

The station-wise annual distribution is further grouped as high and low-value regions of IPWV on an annual basis over Indian regions (Table- 2 & Fig. 4). The annual high IPWV region are found in the coastal regions, with mean IPWV ranging from 43.28 mm (over Machilipatnam) to 47.59 mm (over Thiruvananthapuram) and over northeast India with a mean IPWV of 43.54 mm (over Dibrugarh). Mean IPWV over central India ranged from 27.01 (Aurangabad) mm to 36.53 mm (Nagpur). The lowest IPWV was expectedly observed over the desert areas of northwest India with an IPWV of about 23.86 mm. The lowest values of the annual mean of IPWV are observed at the desert station Sriganganagar (23.86 mm) and the highest ones at the station on the Thiruvananthapuram (47.59 mm) at the west coast of India. Dwarka, though a coastal station, located at the extreme northern part of the west coast of India recorded a low value of 26.69 mm annual mean IPWV primarily because of the incursion of dry winds from the desert regions of Pakistan and Afghanistan. This distribution corresponds to high mean annual surface temperature and means high relative humidity over the coastal stations (Table-2 & Fig. 4).

Table-2: Annual Mean IPWV, T_{sur} & RH

S.No.	Stations Name	Station Code	Annual		
			IPWV(mm)	T_{sur} (°C)	RH (%)
1	Jaipur	JIPR	24.27	24.91	46.18
2	Raipur	RIPR	29.52	26.79	53.20

3	Thiruvananthapuram	TRVM	47.59	27.17	74.49
4	Karaikal	KRKL	44.67	29.06	69.85
5	Kanyakumari	KYKM	44.99	27.56	74.85
6	Machilipatnam	MPTM	43.28	27.90	70.79
7	Jalpaiguri	JPGI	36.96	23.01	74.20
8	Dwarka	DWRK	26.69	26.51	69.43
9	Jabalpur	JBPR	31.03	24.72	60.10
10	Sriganganagar	SGGN	23.86	23.68	56.74
11	Delhi	DELH	27.55	24.01	57.67
12	Pune	PUNE	34.03	25.27	65.00
13	Nagpur	NGPR	36.53	27.07	52.37
14	Panjim	PNJM	47.46	27.27	64.24
15	Aurangabad	ARGD	27.01	26.44	44.51
16	Dibrugarh	DBGH	43.54	23.72	77.54

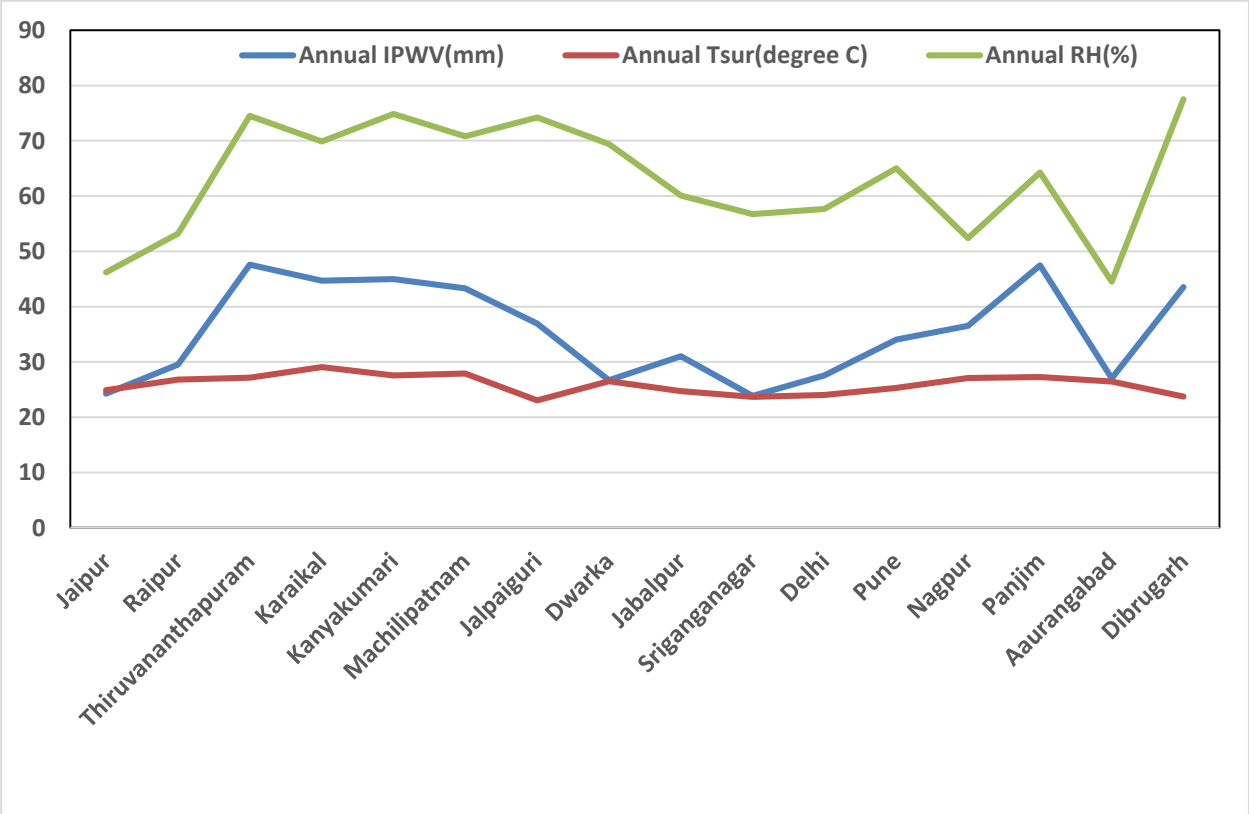

Fig. 4 Annual mean values of IPWV (mm), T_{sur} (ºC) and RH (%)

3.2 Seasonal and Monthly Variation

Average seasonal values of IPWV are determined by the combined effect of average seasonal temperatures and moisture transport by large-scale flow patterns. IPWV values averaged over different seasons are given in Table 3 and Fig. 5 below. Controlled by low temperatures, reduce the evaporation from the ground and dominance of dry continental air mass, the lowest seasonal values of IPWV (Sri Ganganagar – 10.57 mm, Jaipur – 10.95 mm, and Delhi – 12,56 mm) are observed over the plains of northwest India during the winter season (Jan-Feb). The highest seasonal values are observed over the coastal stations (Thiruvanatpuram - 36.5 mm, Kanyakumari - 35.4 mm, and Karaikal - 30.2 mm) on account of relatively higher temperatures and due to proximity to the sea. The lowest average winter season IPWV values during the winter season (and also during pre-monsoon and post-monsoon seasons) among the coastal stations were found over Dwarka as the region is dominated by dry northerly winds from the dry regions of Pakistan and Afghanistan. A general increase across the stations is found during the following season (pre-monsoon) with the highest values over the coastal stations and the lowest over the inland stations. The evaporation rate during the summer months increases due to higher surface temperature (T_{sur}) values and it causes the water vapour to concentrate in the atmospheric layers consequently increasing the IPWV (Fig. 5). In contrast, winter months with low surface temperature reduce the evaporation from the ground and hence reduction in IPWV. Average IPWV continue to increase reaching their seasonal maximum in the monsoon season. Also, the lowest variation across the regions was found during the monsoon season owing to the dominance of maritime monsoon air mass over the country. Most of the stations record average seasonal values between 50 mm and 60 mm. Values in excess of 60 mm were found over the heavy rainfall stations in the northeast of the country – Jalpaiguri, and Dibrugarh. IPWV values fall in the post-monsoon season (Oct-Dec) with the withdrawal of southwest monsoon from the country. The coastal stations (Thiruvananthpuram, Karaikal, Kanyakumari, and Panjim), however, continue to have higher values during the post-monsoon season also.

Table-3: Seasonal Mean IPWV

S.No.	Stations Name	Pre-monsoon	Post-monsoon	Monsoon	Winter
1	JIPR	20.79	25.63	52.65	10.94
2	RIPR	24.87	36.10	58.07	14.18

3	TRVM	47.38	52.82	53.51	36.46
4	KRKL	39.48	50.57	55.37	30.20
5	KYKM	43.70	52.36	50.75	35.37
6	MPTM	37.29	46.20	60.73	25.40
7	JPGI	38.19	40.24	66.16	19.44
8	DWRK	19.81	29.82	51.88	13.71
9	JBPR	20.91	32.71	57.68	13.33
10	SGGN	21.70	24.87	48.49	10.57
11	DELH	22.80	28.40	55.68	12.56
12	PUNE	21.54	32.99	49.62	16.23
13	NGPR	24.74	40.60	58.47	17.33
14	PNJM	39.84	49.72	55.37	29.68
15	ARGD	21.26	35.93	50.44	16.38
16	DBGH	35.56	52.02	66.44	20.15

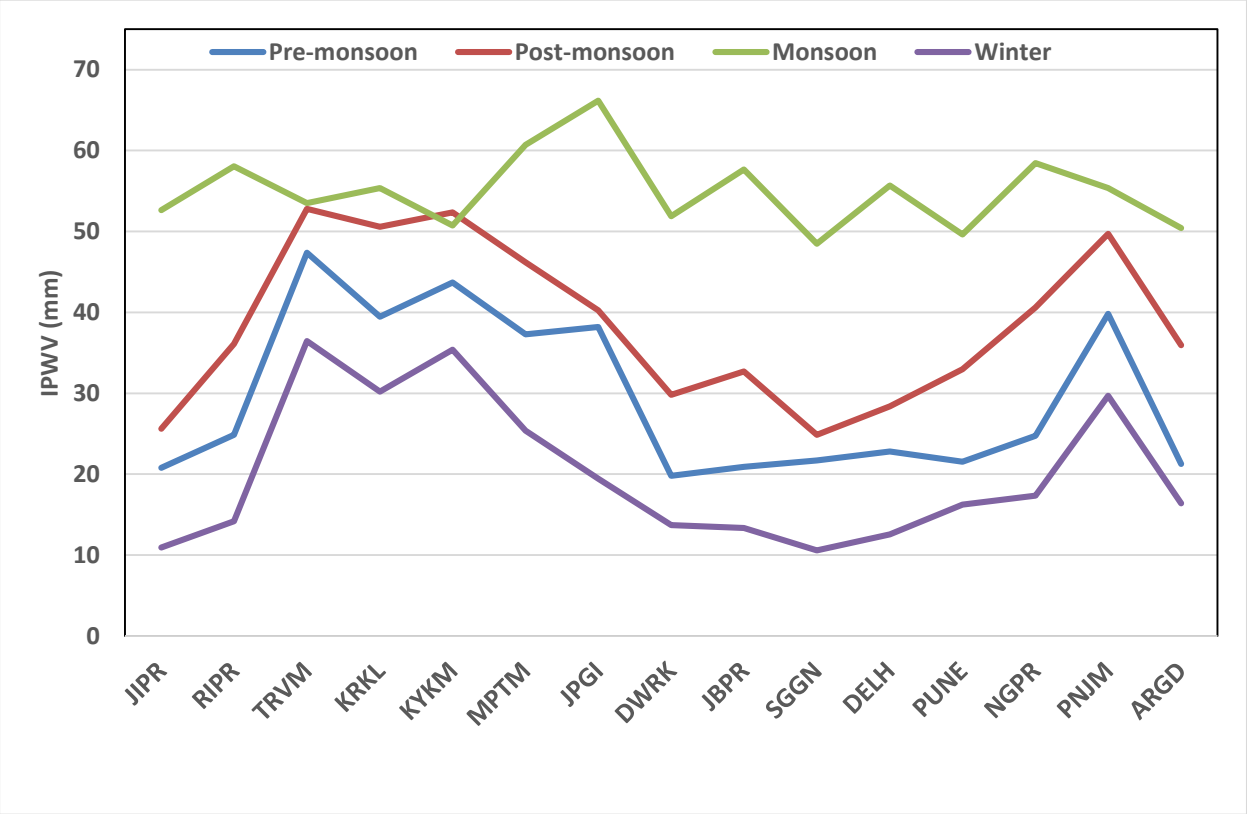

Fig. 5 Seasonal mean values of IPWV (mm)

IPWV is a function of the total water holding capacity of the atmosphere governed by the Clausius–Clapeyron equation; and thus, rises with increases in temperature. Given the supply of moisture over a region, the warmer season has higher IPWV than a colder season. With every 1°C increase in global temperature, an increase of about 7% in atmospheric water vapour has been reported by Trenberth et al. (2003). In India, dry winters are followed by summer and then the rainy season. The IPWV accordingly exhibits a gradual increase from winter to monsoon season through the pre-monsoon season and then a gradual decrease up to the winter season which can be attributed to the variation in the water holding capacity of air governed by the variation in temperature and to the synoptic features of the summer monsoon. In coastal stations, the relative humidity is always higher compared to the inland stations (Fig. 5 & Table. 3).

Station-wise monthly mean distribution of IPWV from January to December (Fig. 6) shows obvious monthly differences. The highest mean monthly values of IPWV were found during the peak of the monsoon season (July/August); whereas the lowest values were found during the dry winter season (December/January), respectively. The highest values of the monthly mean distribution of IPWV values over the inland stations ranged from 51.6 mm at Pune to 69.5 mm at Jalpaiguri. The lowest values ranged from 8.8 mm over Jabalpur to 17 mm over Jalpaiguri. Mean values of maximum IPWV during monsoon months over the stations in the relatively low rainfall desert region of Rajasthan (Jaipur and Sri Ganganagar) were either comparable or higher than that over other stations. This is primarily because of the presence of anti-cyclonic circulation between 1.5 and 4 km which has an inhibiting effect on precipitation over the region (Koteshwaram, 1968; Rakhecha, 2018).

The mean monthly values of IPWV over coastal stations were generally higher than those of the inland stations with the maxima found till late in the season – August. Some of the stations over the west coast also have a secondary maximum in the month of October associated with the northeast monsoon. The highest monthly mean IPWV over the coastal stations ranged from 55 mm over Kanyakumari and Dwarka to 61 mm over Machilipatnam. The lowest values of IPWV ranged from 13 mm over Dwarka to 32 mm over Thiruvananthapuram.

Aurangabad

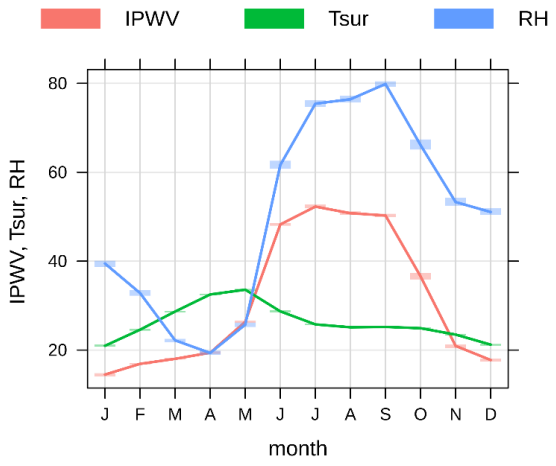

Delhi

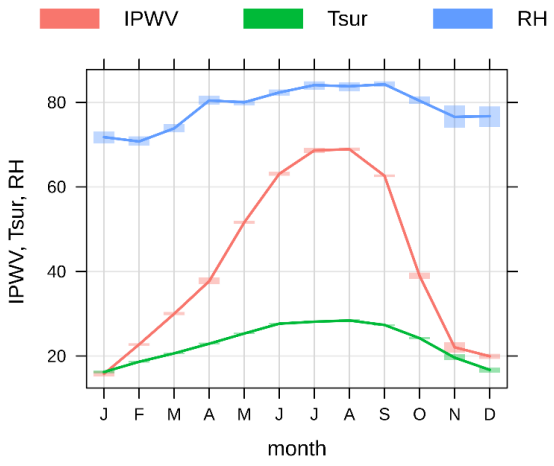

Dwarka

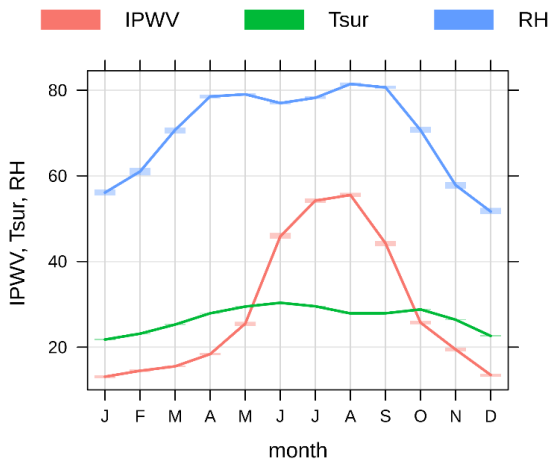

Jabalpur

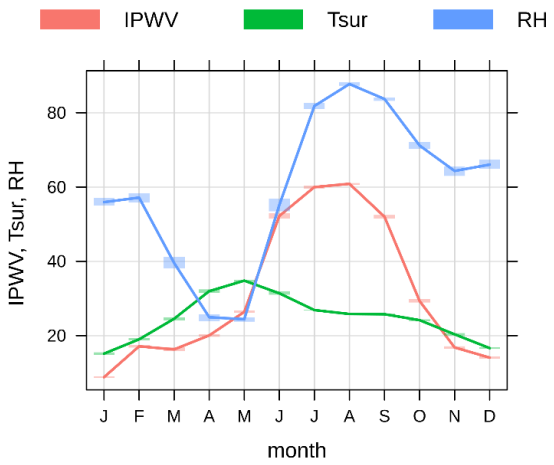

Karaikal

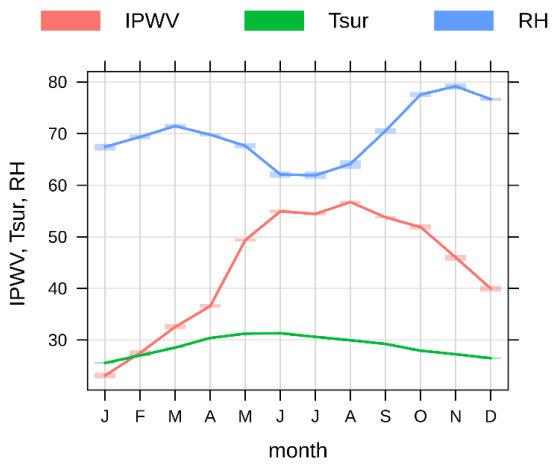

Thiruvanathapuram

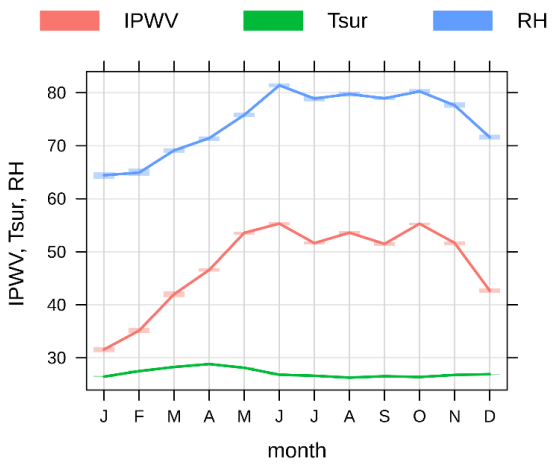

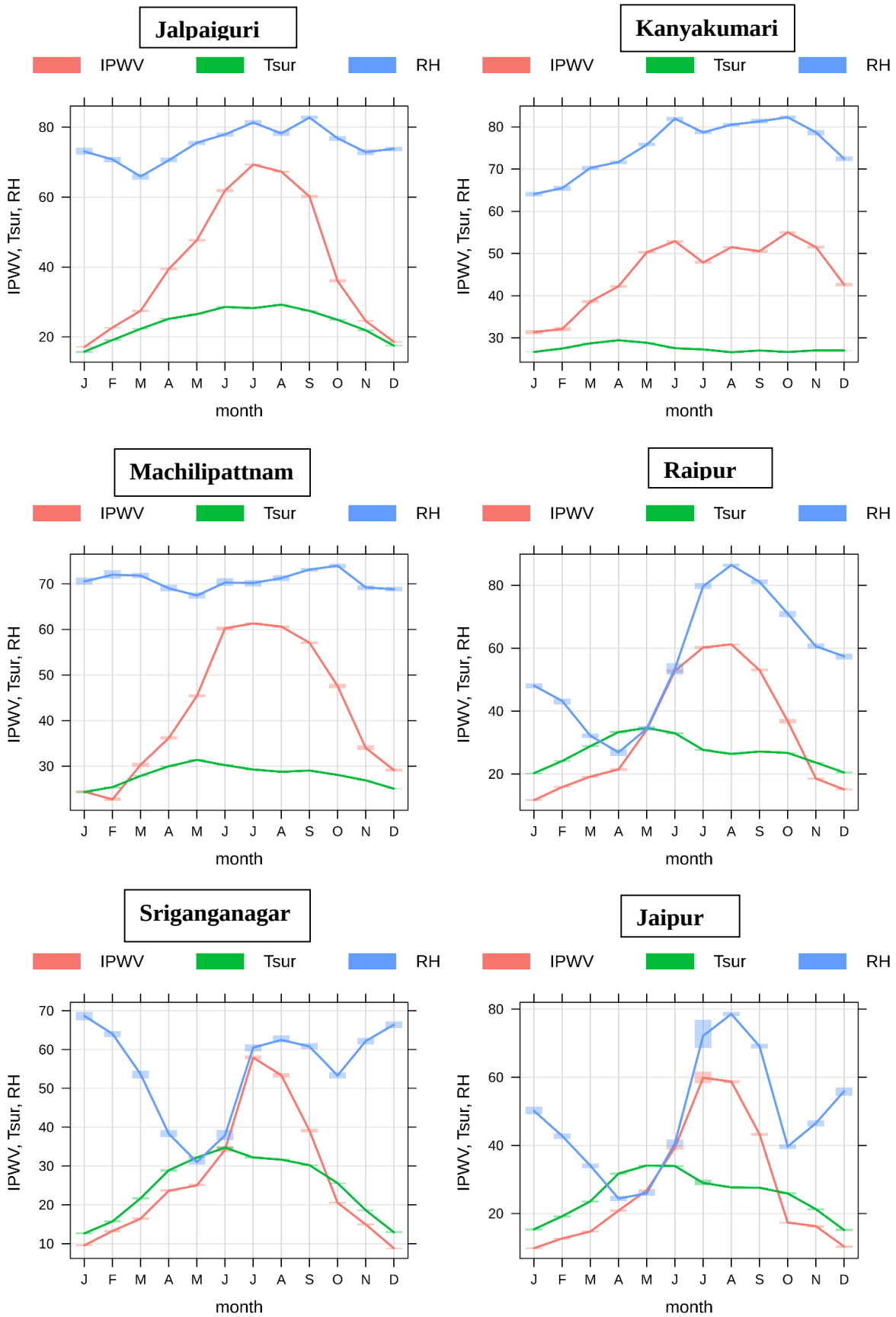
Jalpaiguri
IPWV
Tsur
RH
IPWV, Tsur, RH
month
Kanyakumari
Machilipattnam
Raipur
Sriganganagar
Jaipur
J F M A M J J A S O N D

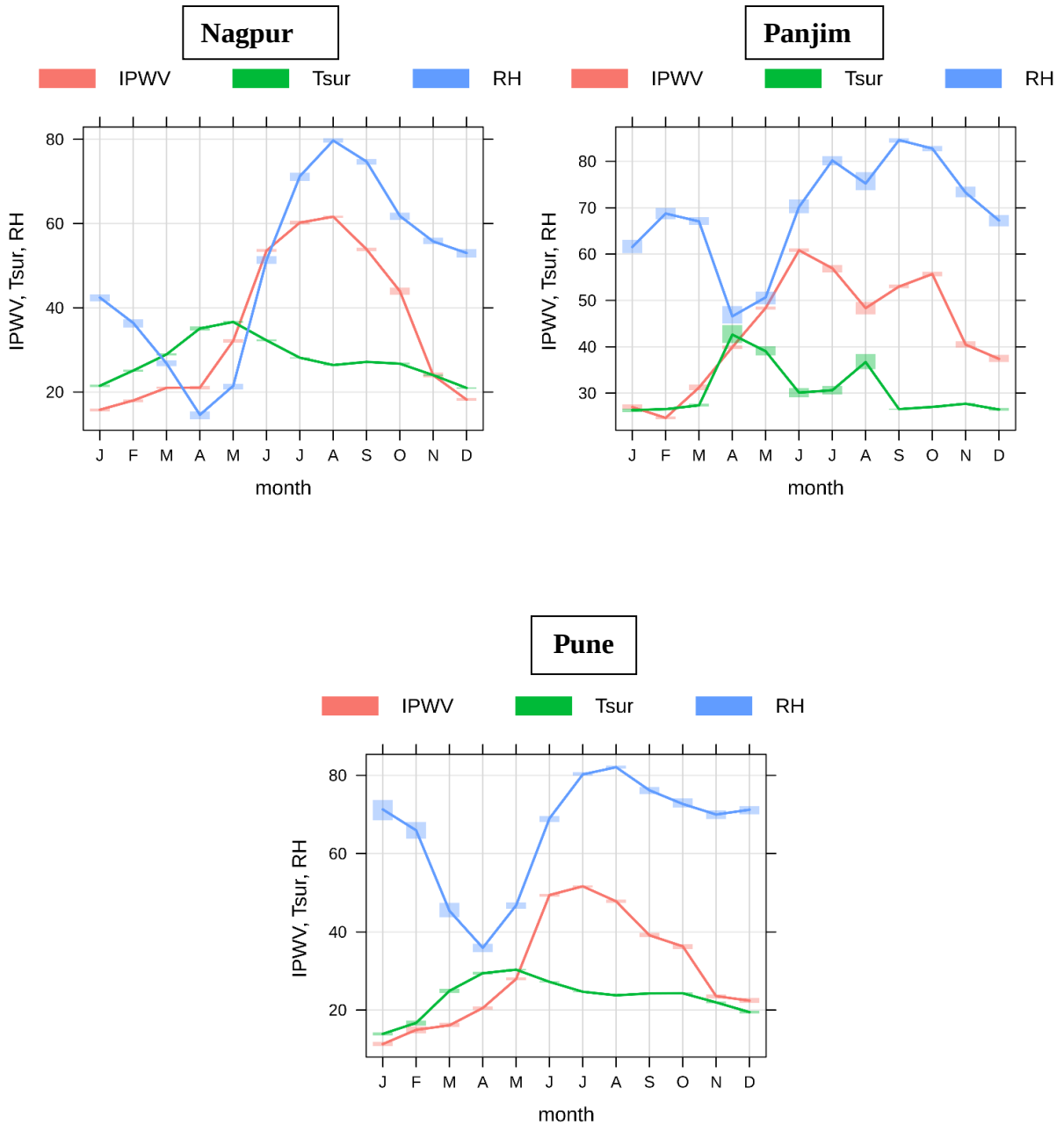

Fig. 6 Monthly Variations of IPWV (mm), Surface temperautre (ºC) and Relative Humidity (%) mean and 95% confidence interval in mean.

3.3 Diurnal Variation of IPWV

The diurnal variation of IPWV is primarily controlled by temperature, evapotranspiration, local wind circulations, condensation & precipitation, and vertical air motion around the station area. The surface temperature increases rapidly and relative humidity (RH) decreases from about 0100-0200 Universal Time Coordinate (UTC) at all the stations (Fig. 7). The increase of surface temperature and decrease of RH is due to intense solar heating of the land surface starting after sunrise, which causes evaporation of water from the surface. The effect of local thermal circulation over the complex topography of India may play a vital role in the diurnal variation of IPWV, such circulation may enhance during daytime as the temperature increases towards late afternoon at all the stations (Fig. 7). These features may lead to an increased circulation late afternoon and evening, start decreasing late evening and night of the day due to weaker circulation and cold surface. The diurnal pattern and time at which the peak of IPWV occurs are station-dependent. The annual mean diurnal variations in IPWV of different stations are shown in Fig. 7 (hours UTC) at the horizontal axis and IPWV in mm as vertical axis). The IPWV values show a clear signature of diurnal variation over all the stations with peak values late evening and midnight and low values during late morning (Fig. 7).

The minimum value of IPWV is reached at early morning hours (0000-0002UTC) at most of the inland stations, slightly later (0002-0004UTC) at the coastal stations except over Dwarka where it was found to occur around 1500 UTC. These are recorded around midnight (1800 UTC) over the desert station - Sri Ganganagar. There is a larger dispersion in the occurrence of maximum values of IPWV, varying from 0800-1000 UTC at inland & dessert stations (Delhi, Jabalpur, Jaipur, Raipur Nagpur, Jalpaiguri, Aurangabad, and Sri Ganganagar); and between 0700-1500 UTC at most of the coastal stations (Fig. 7).

The lowest range of diurnal IPWV values is observer over the inland and desert stations (Delhi, Jabalpur, Jaipur, Raipur Nagpur, Jalpaiguri, Pune, Aurangabad, and Sriganganagar) whereas the maximum diurnal range is observed at the coastal stations (Thiruvanthapuram, Karaikal, Kanyakumari, and Panjim) except Dwarka. Temperature is the most important parameter which plays a crucial role in diurnal warming-derived evaporation, which increases the IPWV. As per Clausius-Clapeyron’s equation, the air can hold more water vapour at higher temperatures, and cooling causes a decrease in the water vapour by condensation. Relative Humidity (RH) is a local measurement and responds to surface temperature, whereas IPWV is an integrated variable that has more weight from the lower troposphere and responds more to horizontal advection or deep convection.

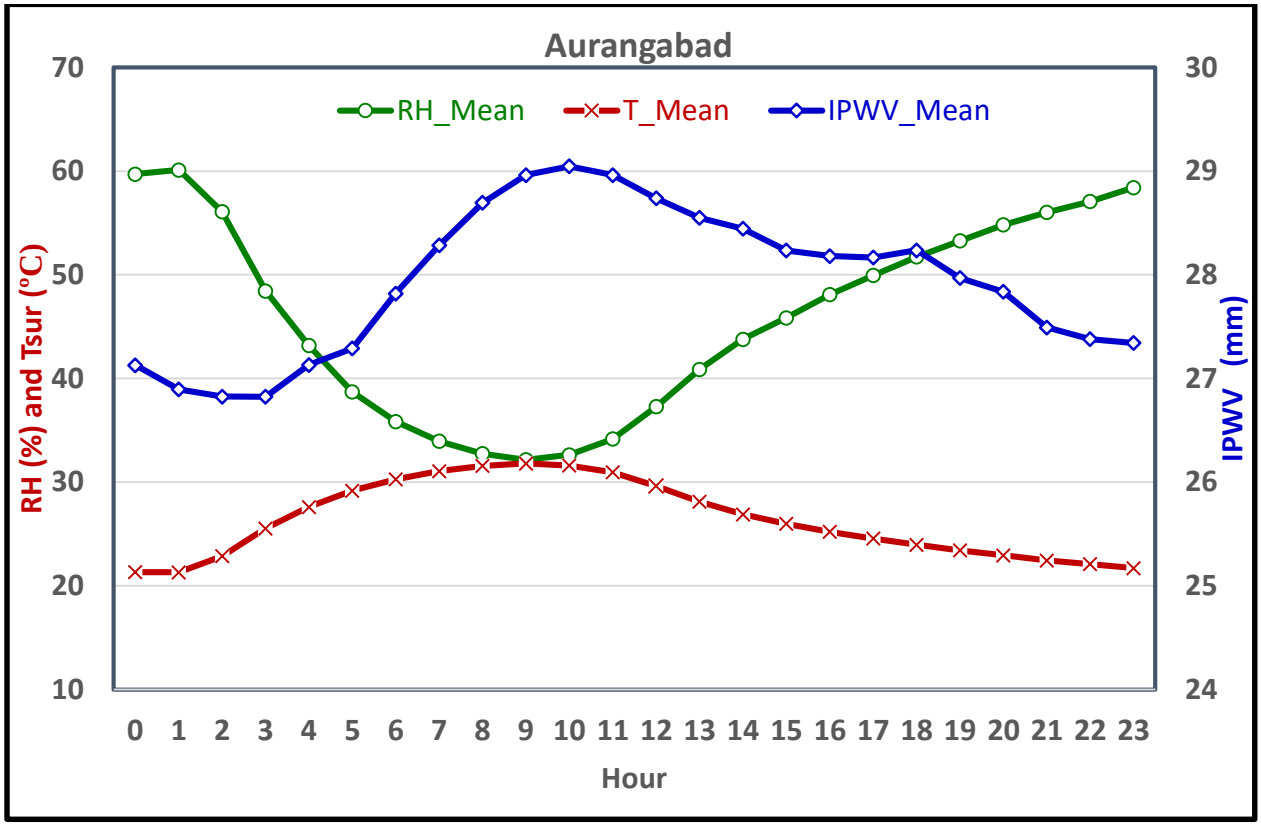
Aurangabad
RH_Mean
T_Mean
IPWV_Mean
RH (%) and Tsur (°C)
IPWV (mm)
Hour
70
60
50
40
30
20
10
30
29
28
27
26
25
24
0 1 2 3 4 5 6 7 8 9 10 11 12 13 14 15 16 17 18 19 20 21 22 23

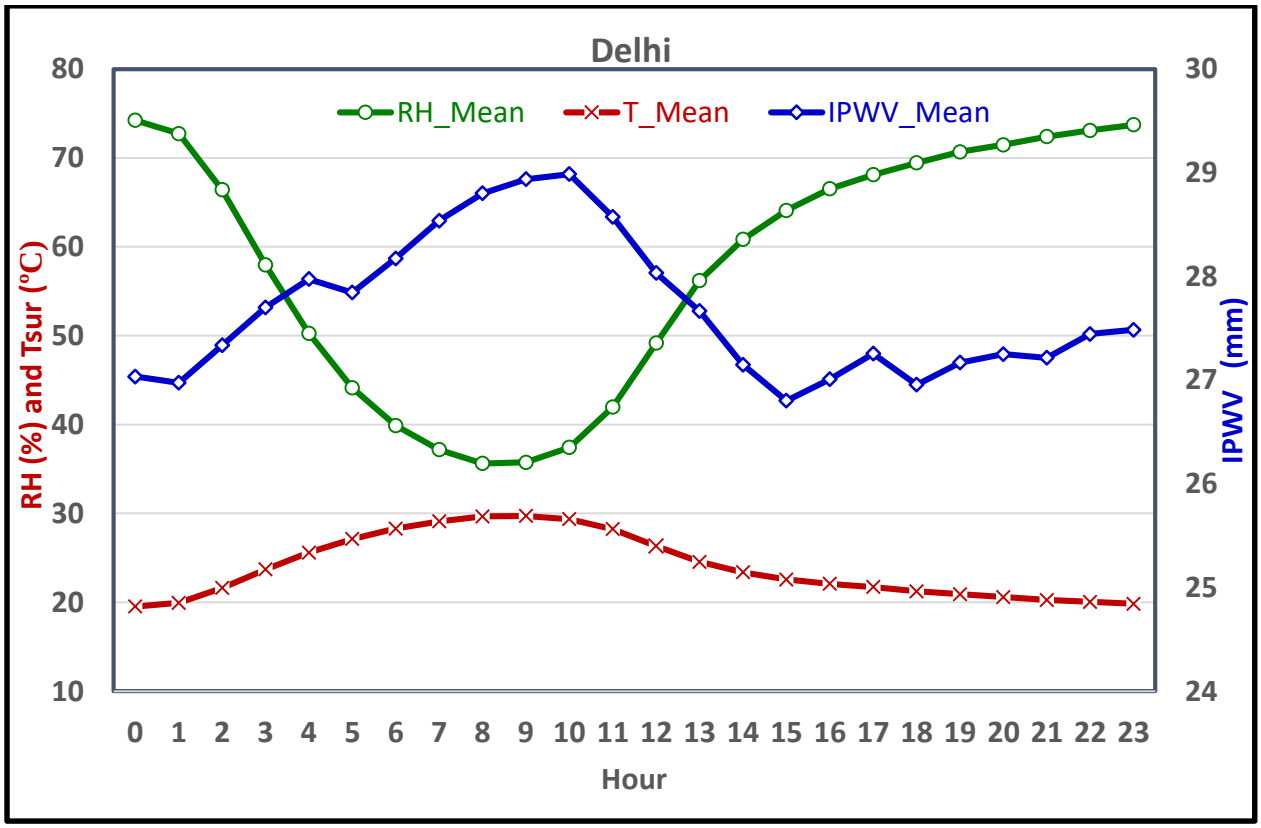
Delhi
RH_Mean
T_Mean
IPWV_Mean
RH (%) and Tsur (°C)
IPWV (mm)
Hour
80
70
60
50
40
30
20
10
30
29
28
27
26
25
24
0 1 2 3 4 5 6 7 8 9 10 11 12 13 14 15 16 17 18 19 20 21 22 23

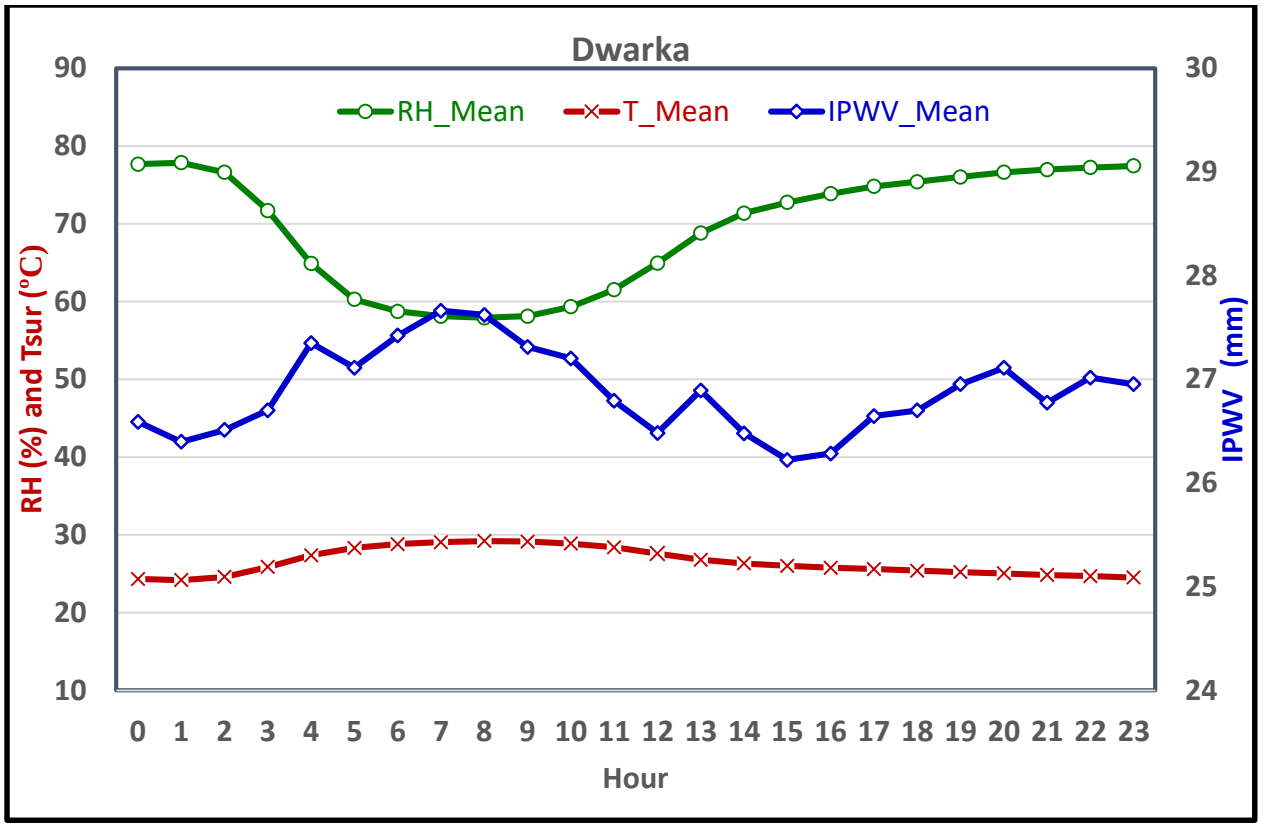
Dwarka
RH_Mean
T_Mean
IPWV_Mean
RH (%) and Tsur (°C)
IPWV (mm)
Hour
90
80
70
60
50
40
30
20
10
30
29
28
27
26
25
24
0 1 2 3 4 5 6 7 8 9 10 11 12 13 14 15 16 17 18 19 20 21 22 23

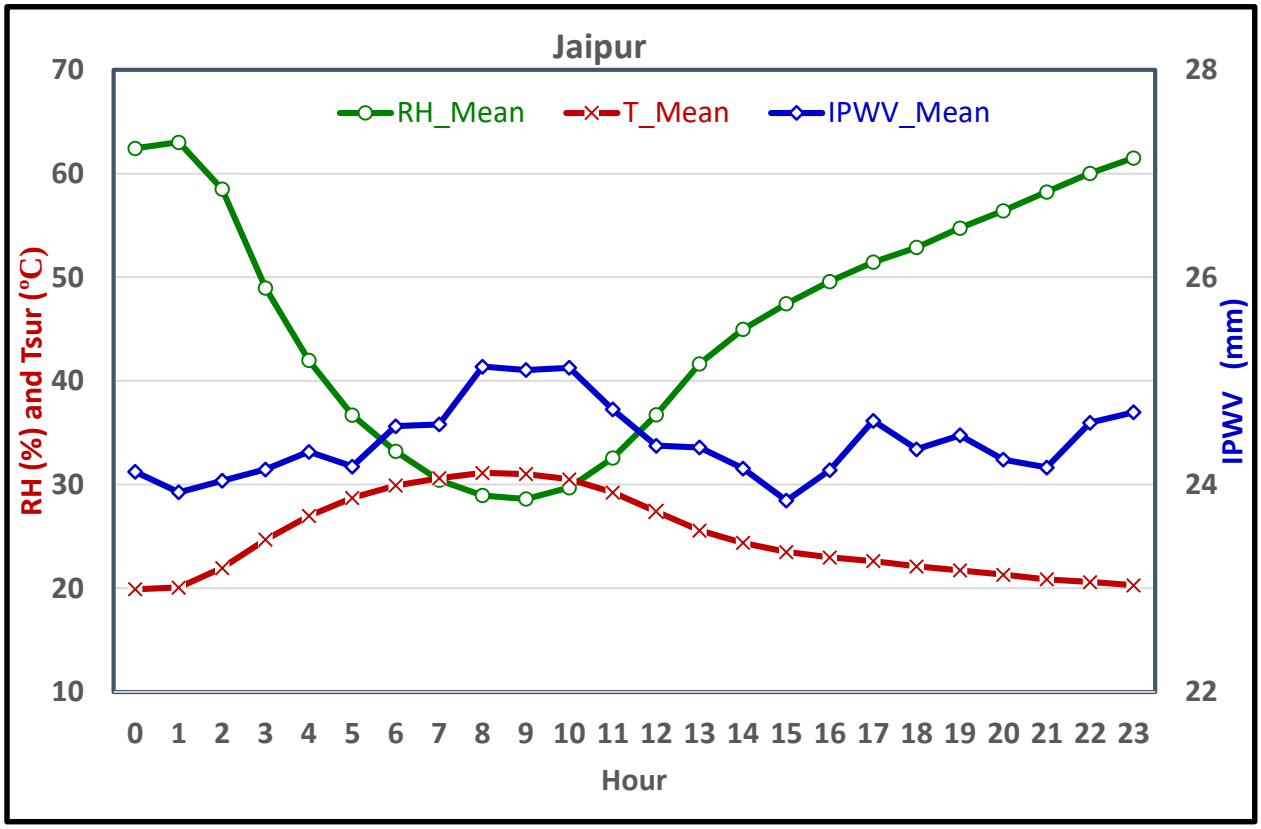
Jaipur
RH_Mean
T_Mean
IPWV_Mean
RH (%) and Tsur (°C)
IPWV (mm)
Hour
70
60
50
40
30
20
10
28
26
24
22
0 1 2 3 4 5 6 7 8 9 10 11 12 13 14 15 16 17 18 19 20 21 22 23

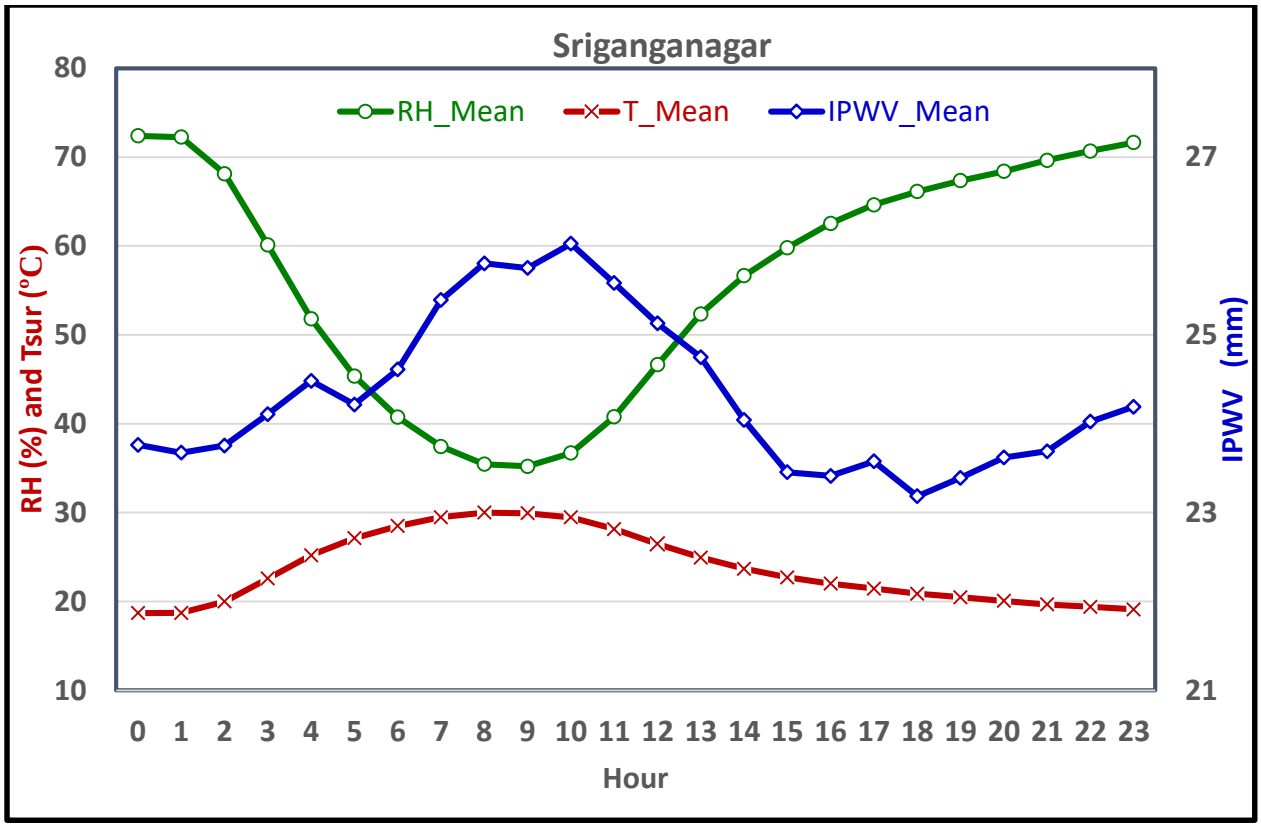
Sriganganagar
RH_Mean
T_Mean
IPWV_Mean
RH (%) and Tsur (°C)
IPWV (mm)
Hour
80
70
60
50
40
30
20
10
27
25
23
21
0 1 2 3 4 5 6 7 8 9 10 11 12 13 14 15 16 17 18 19 20 21 22 23

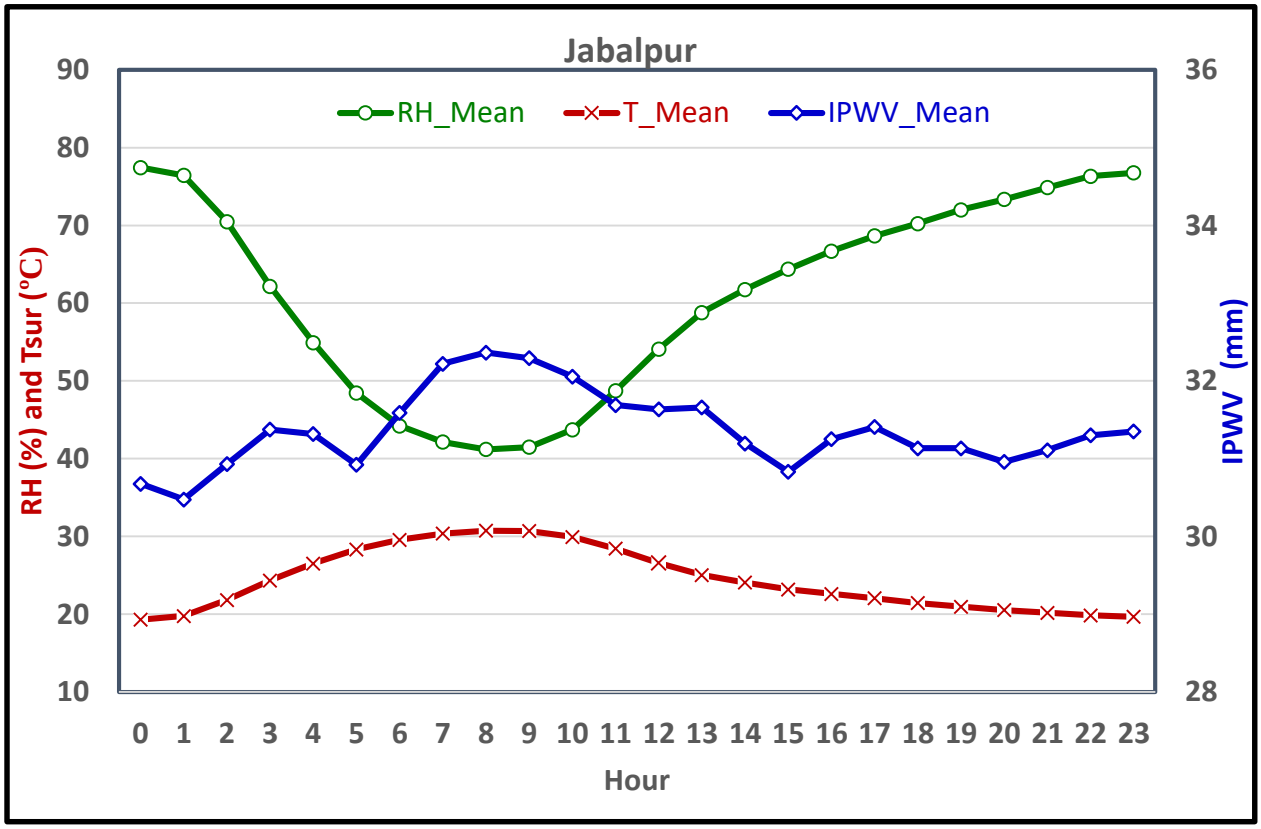
Jabalpur
RH_Mean
T_Mean
IPWV_Mean
RH (%) and Tsur (°C)
IPWV (mm)
Hour
90
80
70
60
50
40
30
20
10
36
34
32
30
28
0 1 2 3 4 5 6 7 8 9 10 11 12 13 14 15 16 17 18 19 20 21 22 23

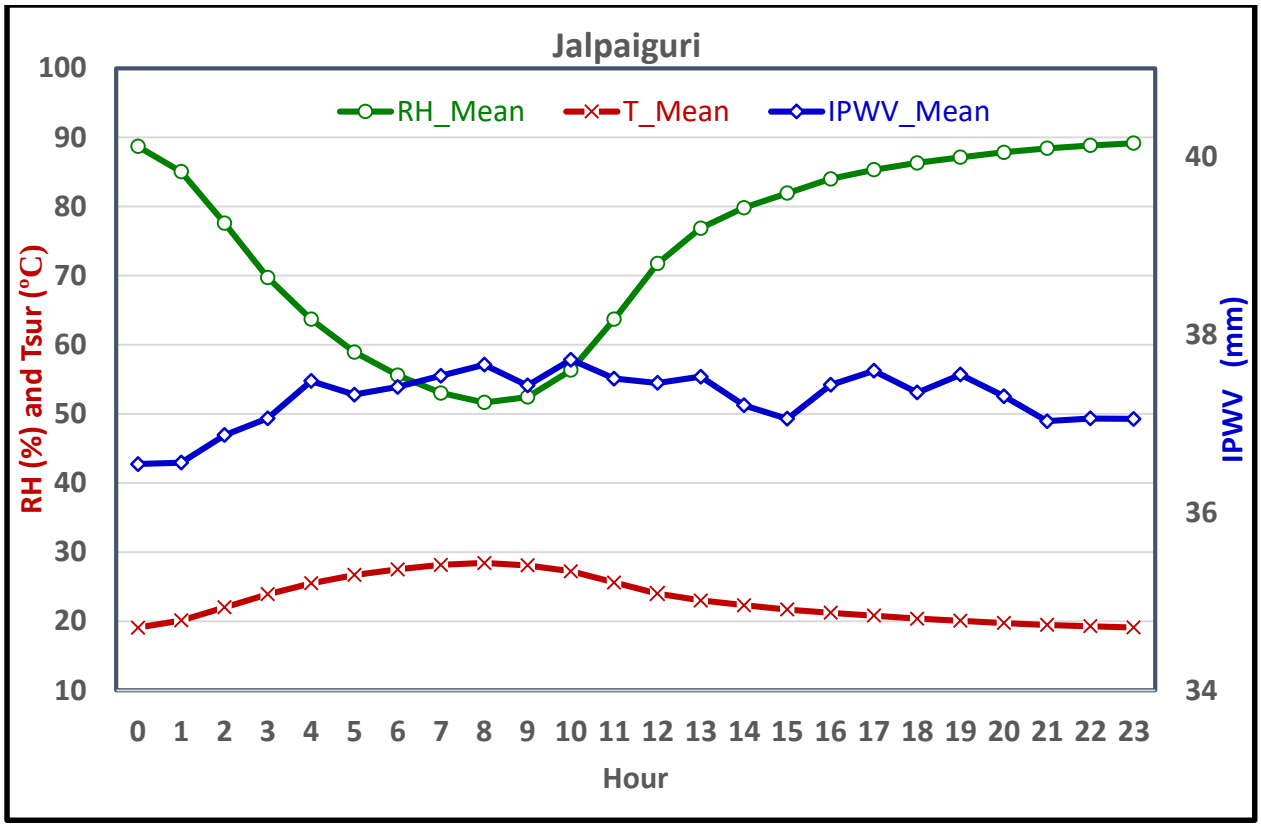
Jalpaiguri
RH_Mean
T_Mean
IPWV_Mean
RH (%) and Tsur (°C)
IPWV (mm)
Hour
100
90
80
70
60
50
40
30
20
10
40
38
36
34
0 1 2 3 4 5 6 7 8 9 10 11 12 13 14 15 16 17 18 19 20 21 22 23

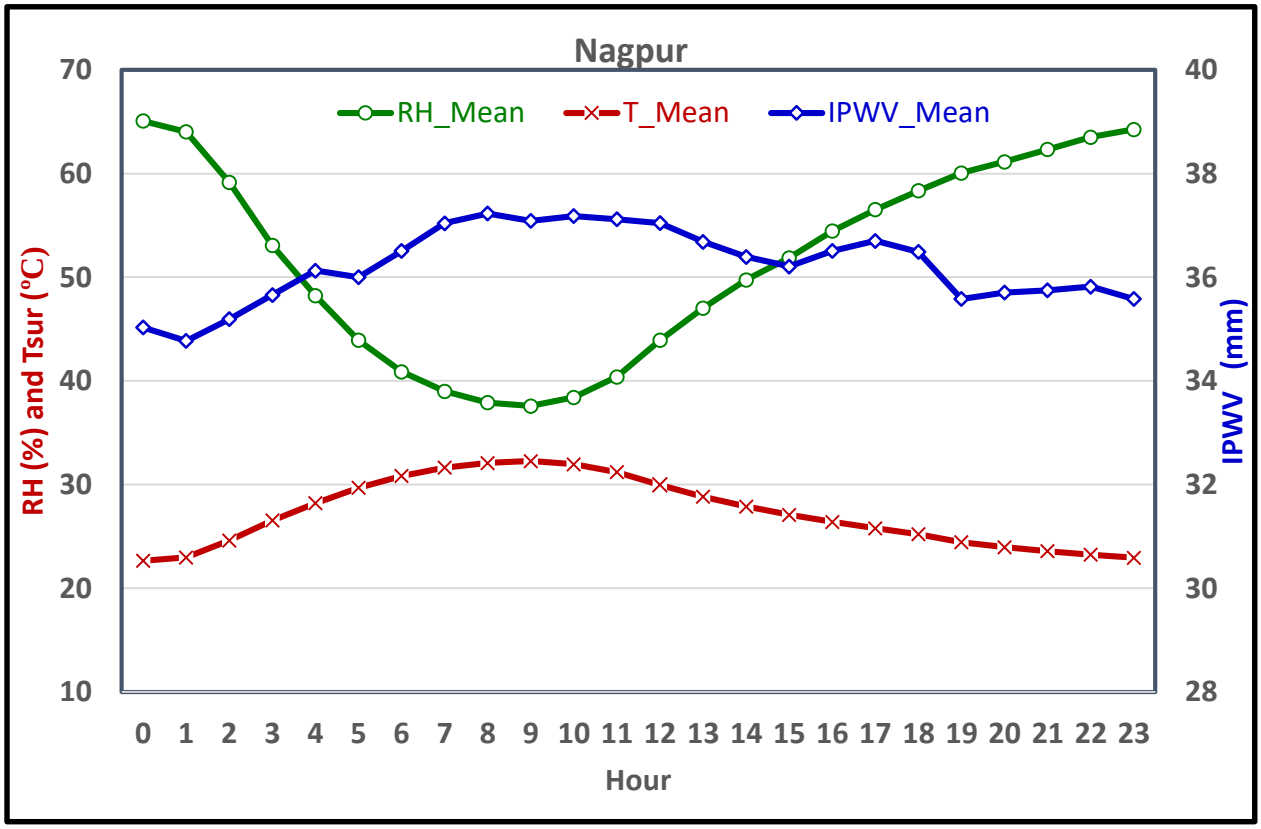
Nagpur
RH_Mean
T_Mean
IPWV_Mean
RH (%) and Tsur (°C)
IPWV (mm)
Hour
70
60
50
40
30
20
10
40
38
36
34
32
30
28
0 1 2 3 4 5 6 7 8 9 10 11 12 13 14 15 16 17 18 19 20 21 22 23

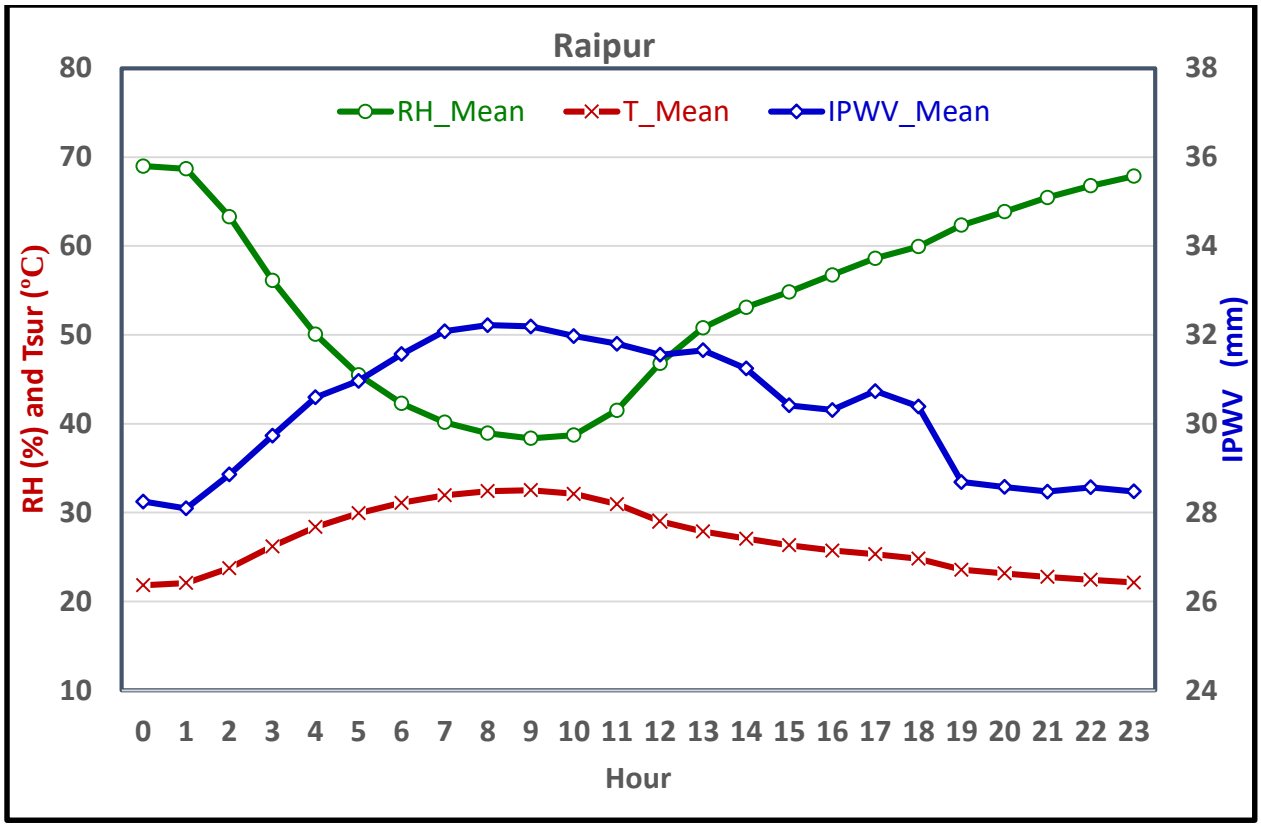
Raipur
RH_Mean
T_Mean
IPWV_Mean
RH (%) and Tsur (°C)
IPWV (mm)
Hour
80
70
60
50
40
30
20
10
38
36
34
32
30
28
26
24
0 1 2 3 4 5 6 7 8 9 10 11 12 13 14 15 16 17 18 19 20 21 22 23

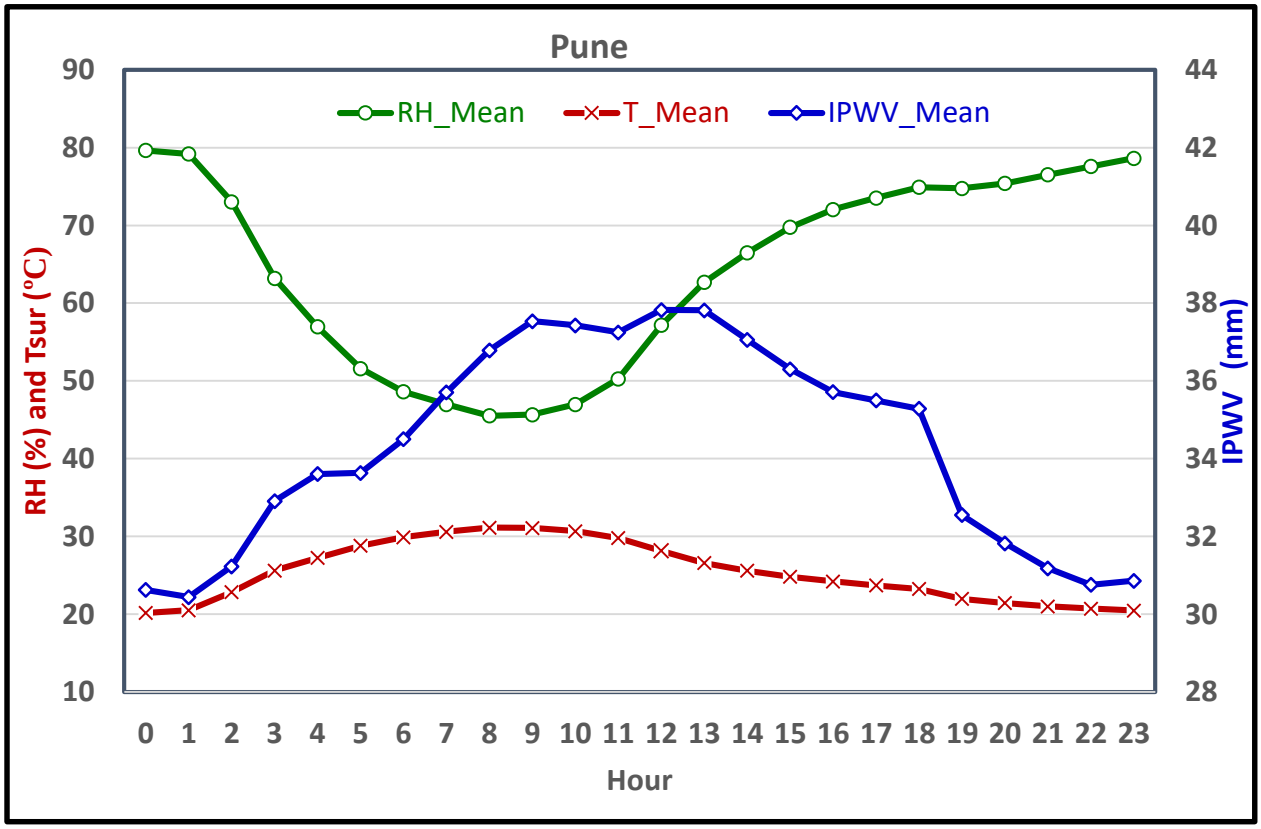
Pune
RH_Mean
T_Mean
IPWV_Mean
RH (%) and Tsur (°C)
IPWV (mm)
Hour
90
80
70
60
50
40
30
20
10
44
42
40
38
36
34
32
30
28
0 1 2 3 4 5 6 7 8 9 10 11 12 13 14 15 16 17 18 19 20 21 22 23

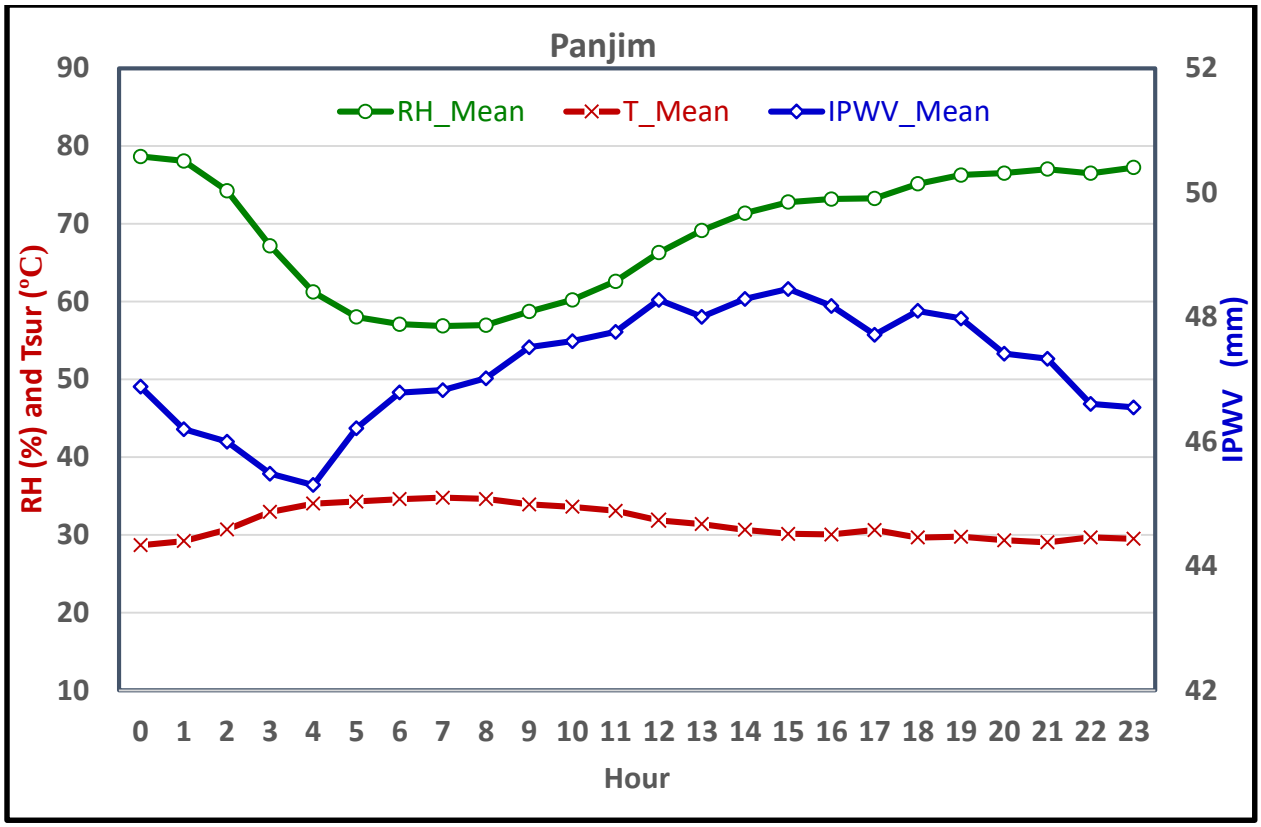
Panjim
RH_Mean
T_Mean
IPWV_Mean
RH (%) and Tsur (°C)
IPWV (mm)
Hour
90
80
70
60
50
40
30
20
10
52
50
48
46
44
42
0 1 2 3 4 5 6 7 8 9 10 11 12 13 14 15 16 17 18 19 20 21 22 23

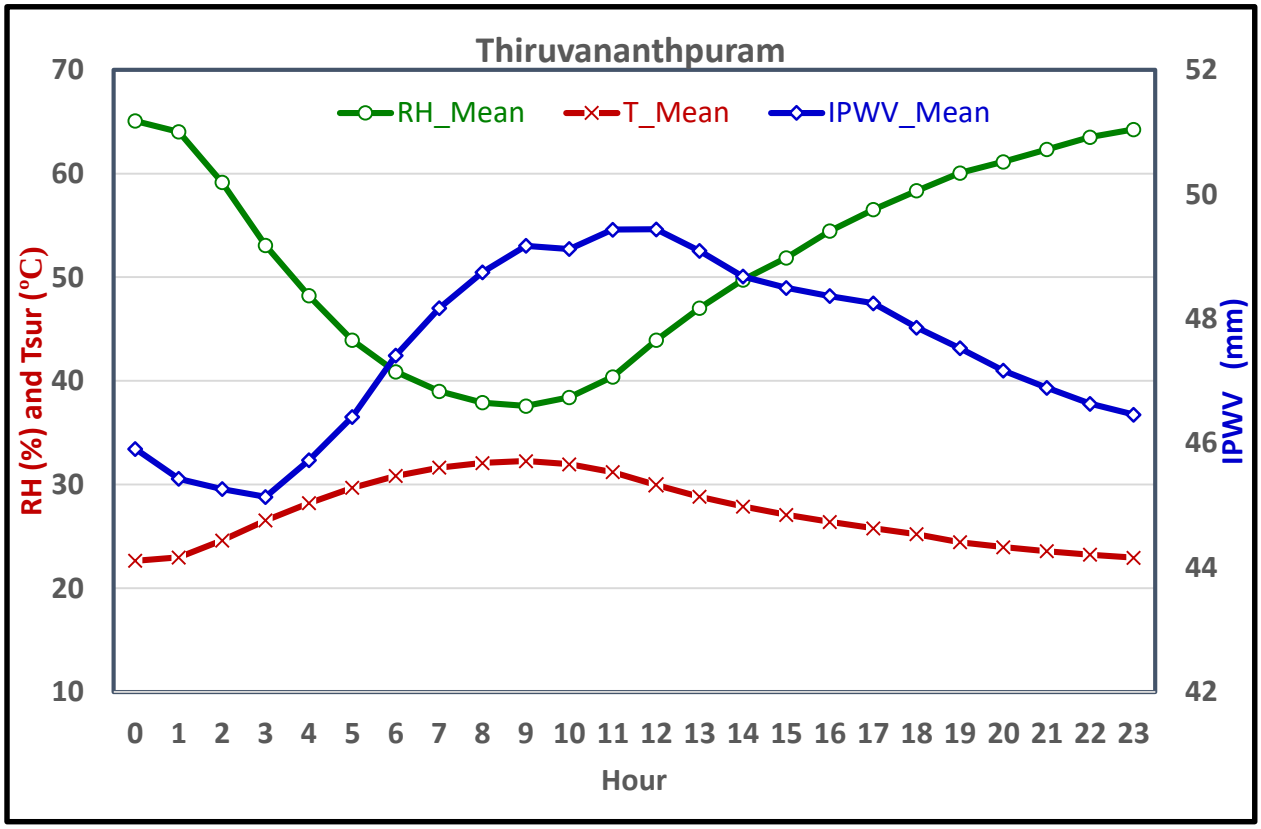
Thiruvananthpuram
RH_Mean
T_Mean
IPWV_Mean
RH (%) and Tsur (°C)
IPWV (mm)
Hour
70
60
50
40
30
20
10
52
50
48
46
44
42
0 1 2 3 4 5 6 7 8 9 10 11 12 13 14 15 16 17 18 19 20 21 22 23

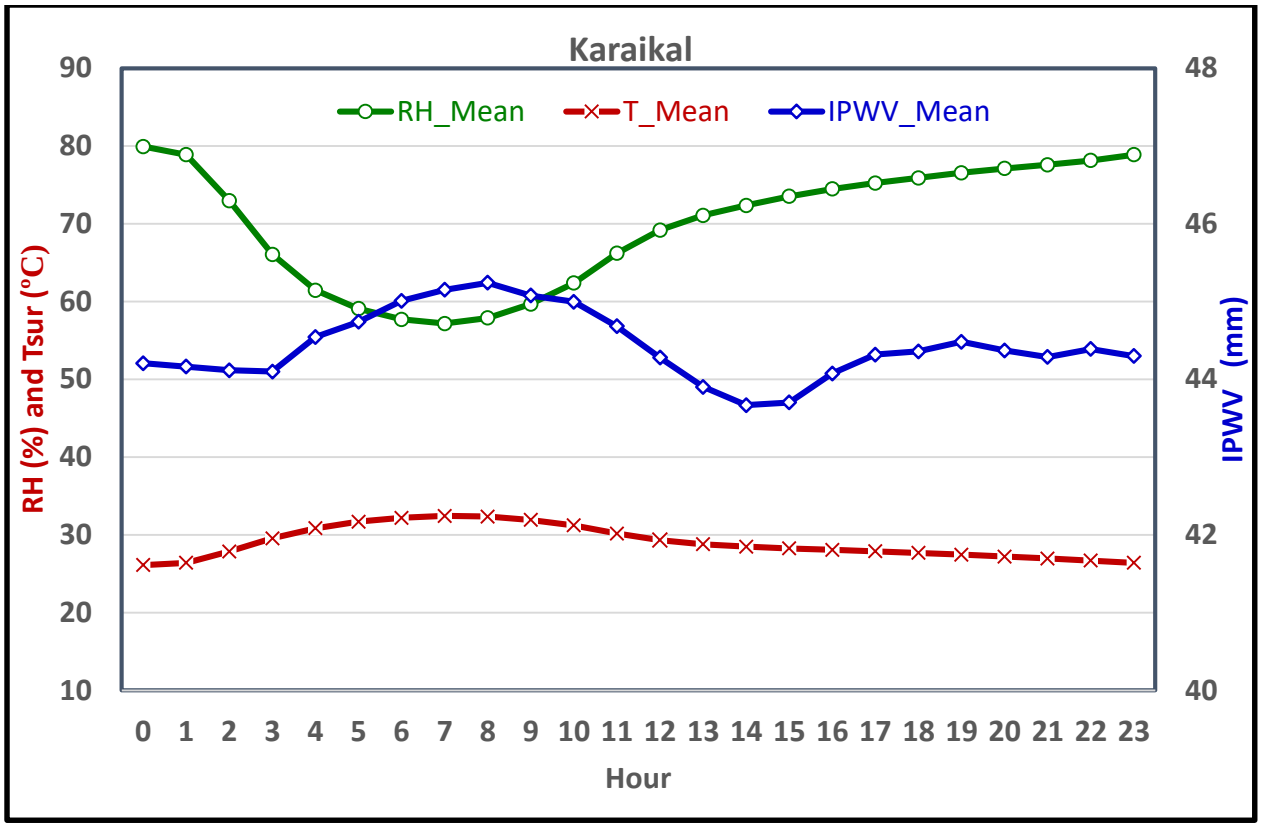
Karaikal
RH_Mean
T_Mean
IPWV_Mean
RH (%) and Tsur (°C)
IPWV (mm)
Hour
90
80
70
60
50
40
30
20
10
48
46
44
42
40
0 1 2 3 4 5 6 7 8 9 10 11 12 13 14 15 16 17 18 19 20 21 22 23

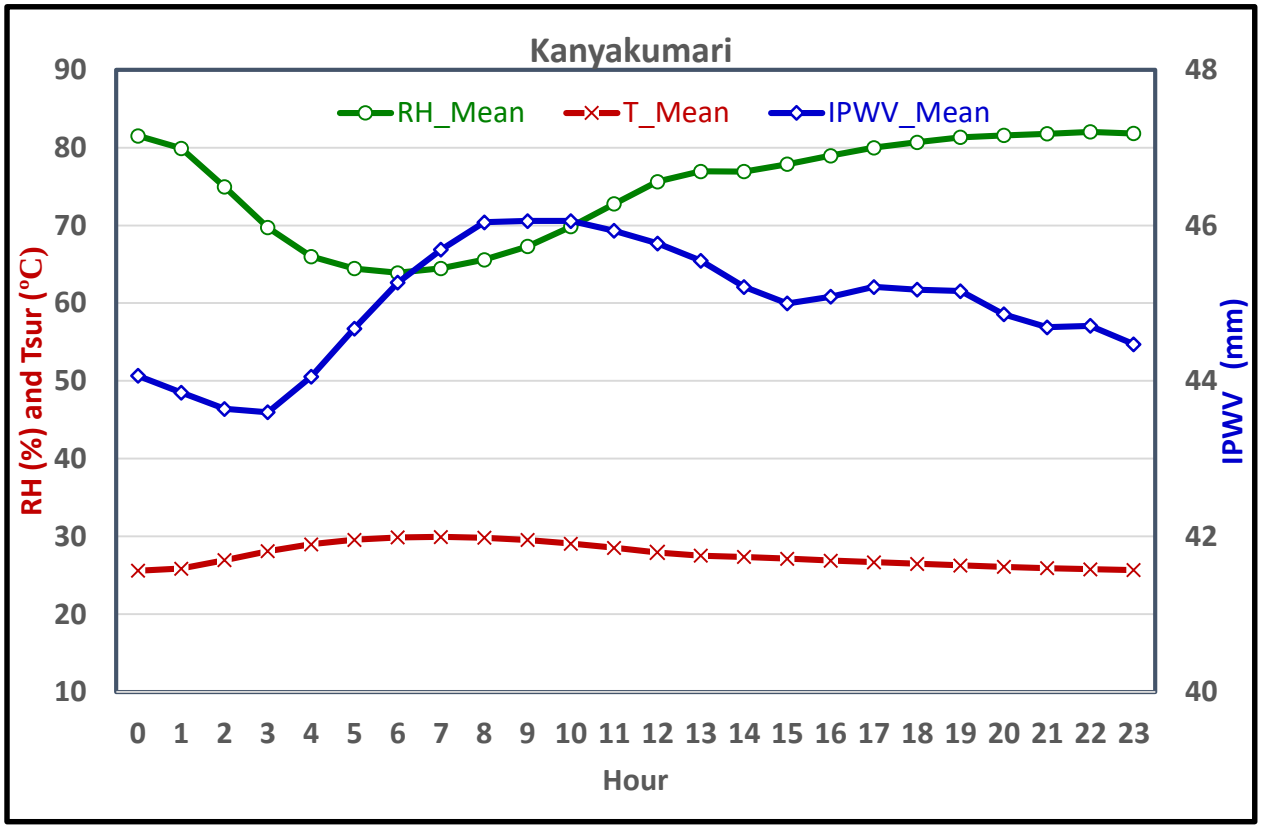
Kanyakumari
RH_Mean
T_Mean
IPWV_Mean
RH (%) and Tsur (°C)
IPWV (mm)
Hour
90
80
70
60
50
40
30
20
10
48
46
44
42
40
0 1 2 3 4 5 6 7 8 9 10 11 12 13 14 15 16 17 18 19 20 21 22 23

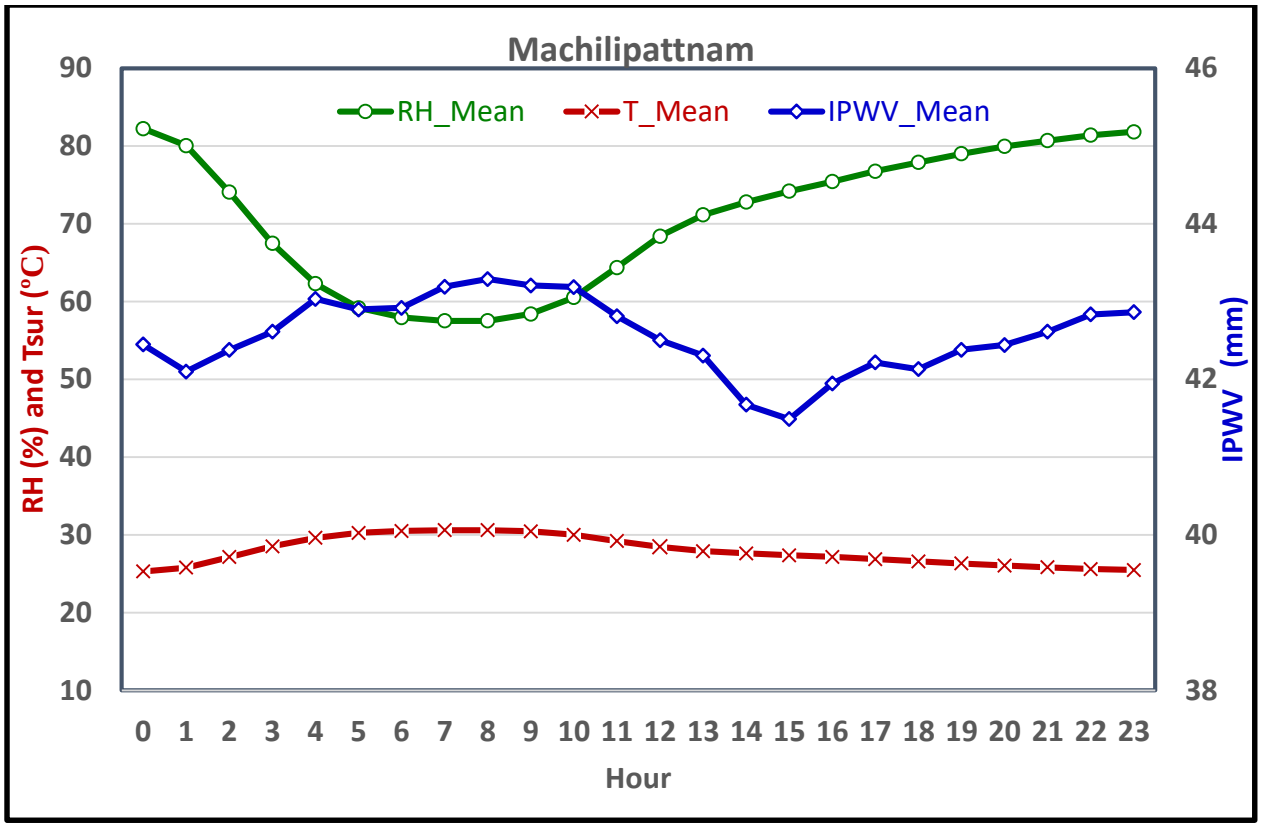

Fig. 7 Diurnal Variations of IPWV (mm), Surface temperature (ºC), and Relative Humidity (%) (mean and 95% confidence interval in mean).

Chapter-4

4.1 Validation of GNSS IPWV with GPS sonde IPWV

GPS-based in situ Radiosonde observations provide the ground truth of atmospheric properties over a station and are used for validation of these properties estimated through remote sensing devices including the GNSS for finding out the errors and biases in these estimates. Validation of GNSS estimated IPWV with in situ GPS Sonde data for the period of June 2017 to May 2018 over the Indian region was carried out for establishing the errors and biases of GNSS IPWV estimates for 9 stations (4 inland and 5 coastal) having continuous observations. The study found reasonably good agreement with a positive bias of less than 4.0 mm for, a correlation coefficient greater than 0.85, and RMSE less than 5.0 mm for all 09 GPS sonde stations. The highest correlation coefficients were observed at two inland stations - Delhi and Nagpur (0.96 and 0.98, respectively) {Fig. 8}. The Correlation coefficients at Raipur, Dibrugarh, and Bhubneshwar were 0.85, 0.90, and 0.94, respectively. The Correlation coefficient at the coastal stations - Karaikal, Panjim, Thiruvananthapuram, and Machilipattnam are 0.86, 0.92, 0.96, and 0.86, respectively. (Fig. 9 & 10). The bias between the GPS Sonde and GNSS values of PWV (Table 4) is less than 4 mm except for Thiruvananthapuram (7.2 mm) and Bhubneshwar (4.94 mm). RMS differences between GNSS PWV and GPS Sonde PWV measurements are less than 5 mm (Table 4). Yadav et al., 2020 reported a relatively larger PWV difference is observed at the coastal stations of India.

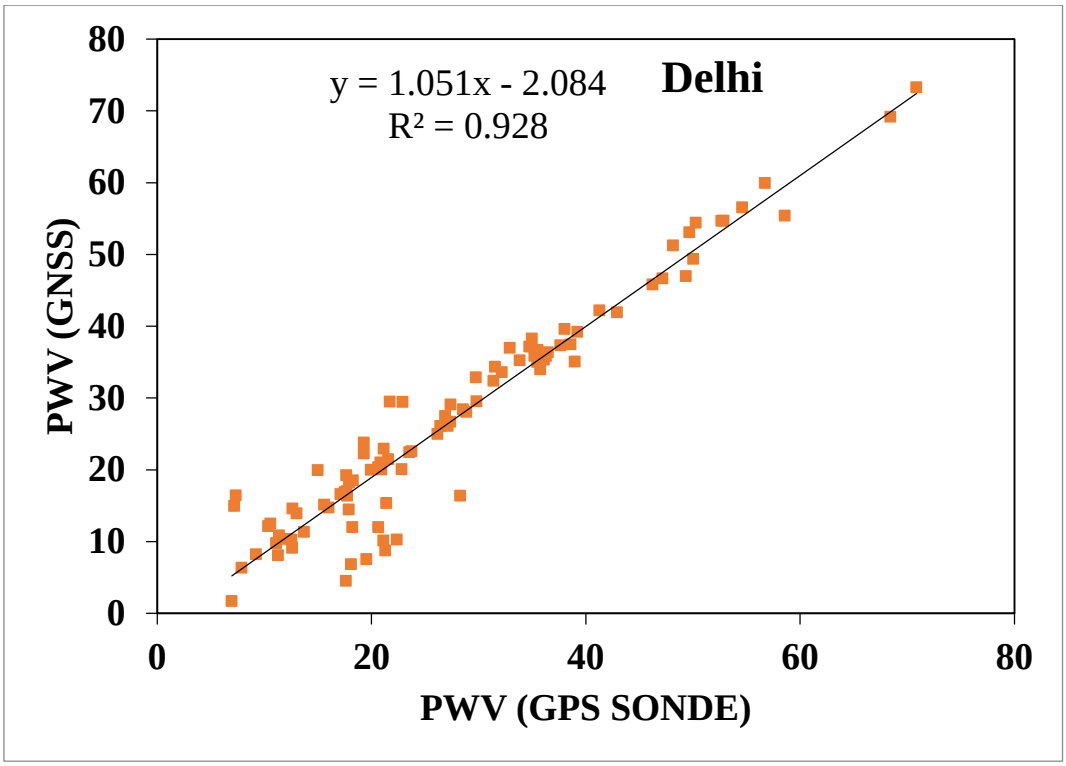

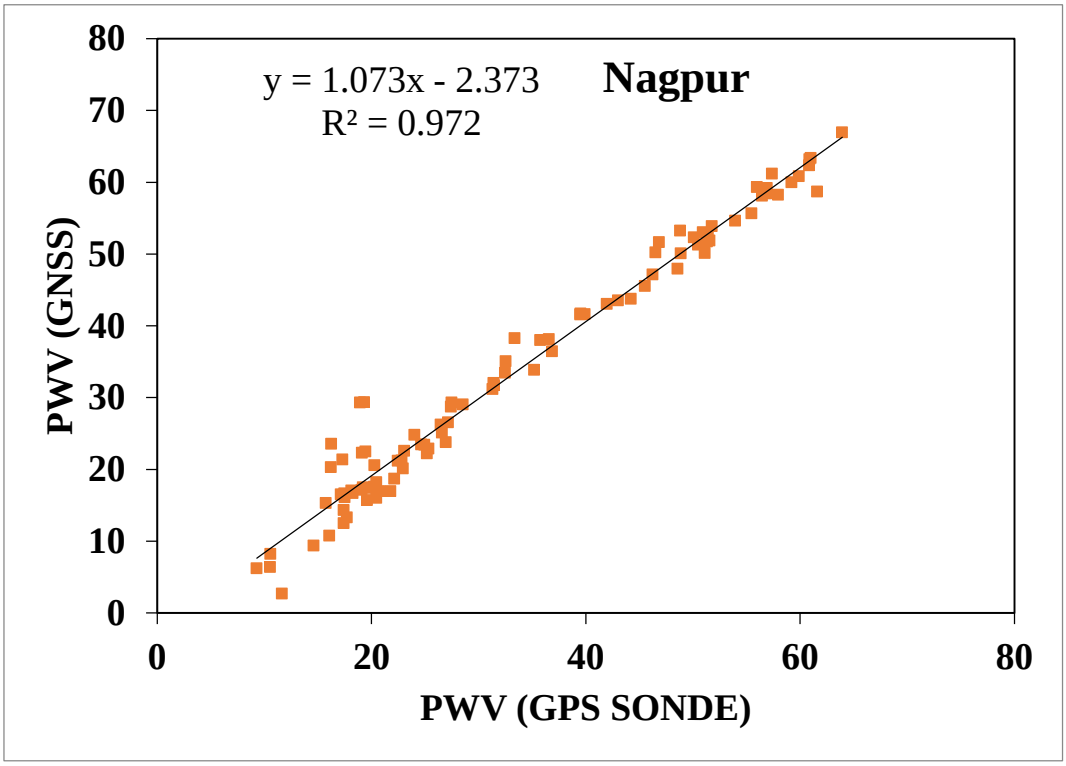

Fig. 8: Scatterplots of GNSS and GPS Sonde PWV (DFM-09 GPS sonde). The correlation coefficient (R) is 96 % for Delhi and 98 % for Nagpur (Yadav et. al., 2020).

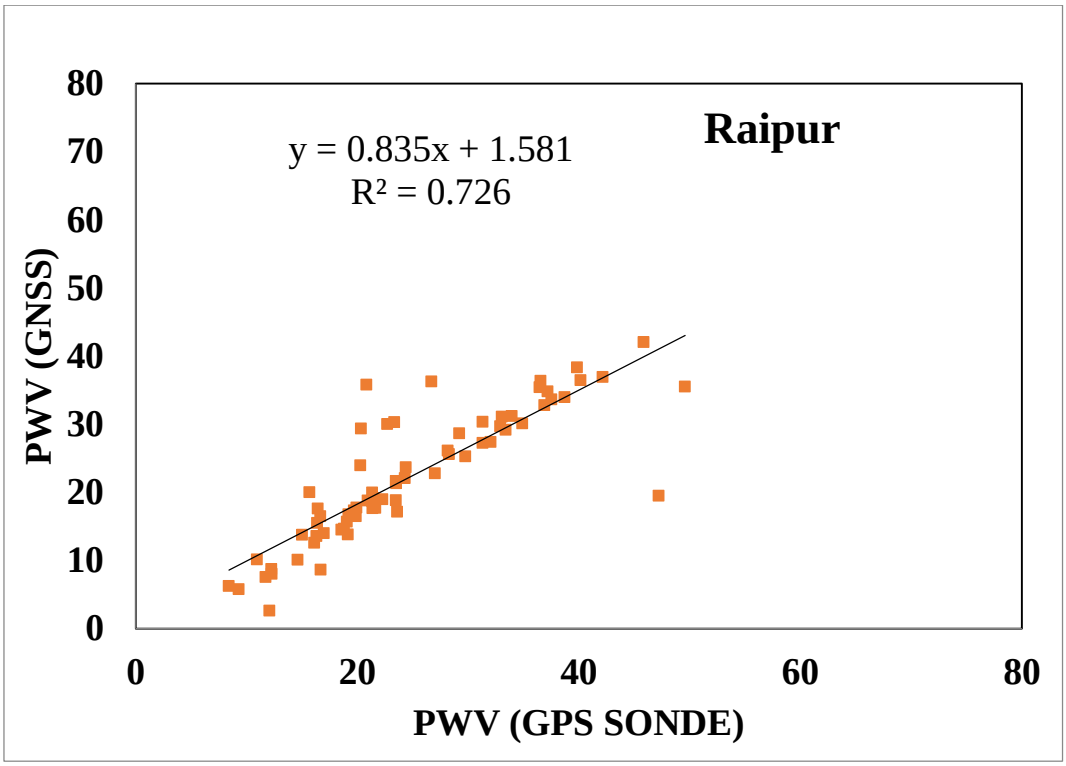
Raipur
y = 0.835x + 1.581
R² = 0.726
PWV (GNSS)
PWV (GPS SONDE)
0
10
20
30
40
50
60
70
80
0
20
40
60
80

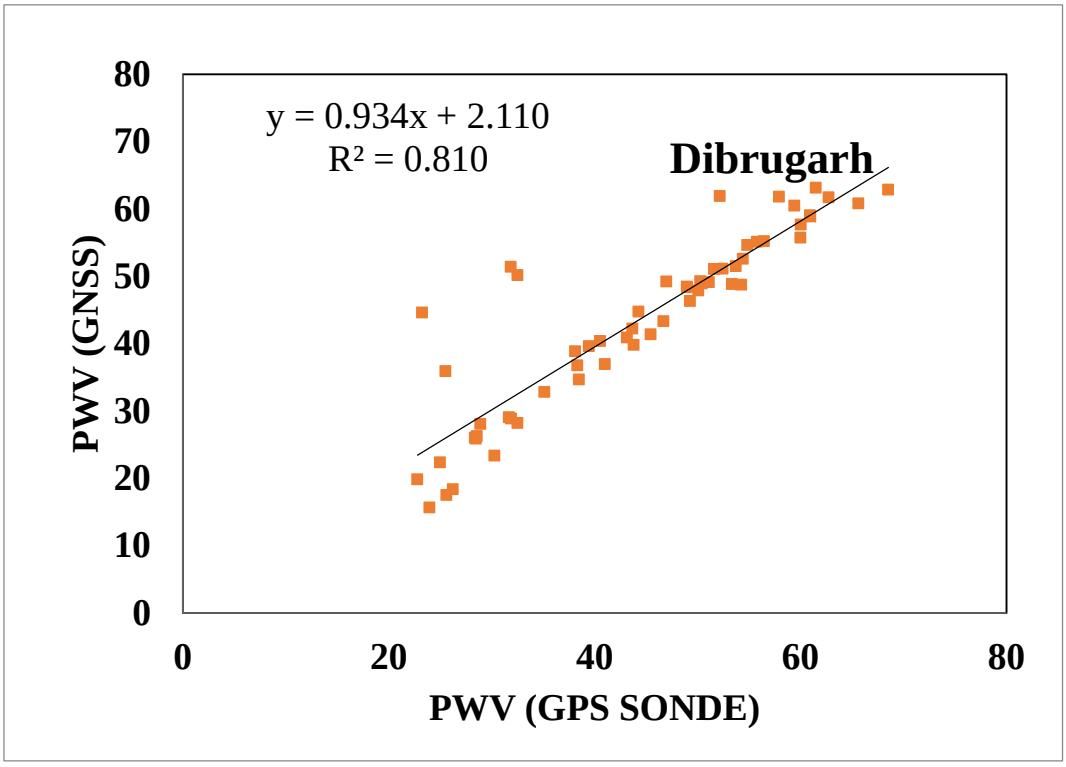
Dibrugarh
y = 0.934x + 2.110
R² = 0.810
PWV (GNSS)
PWV (GPS SONDE)
0
10
20
30
40
50
60
70
80
0
20
40
60
80

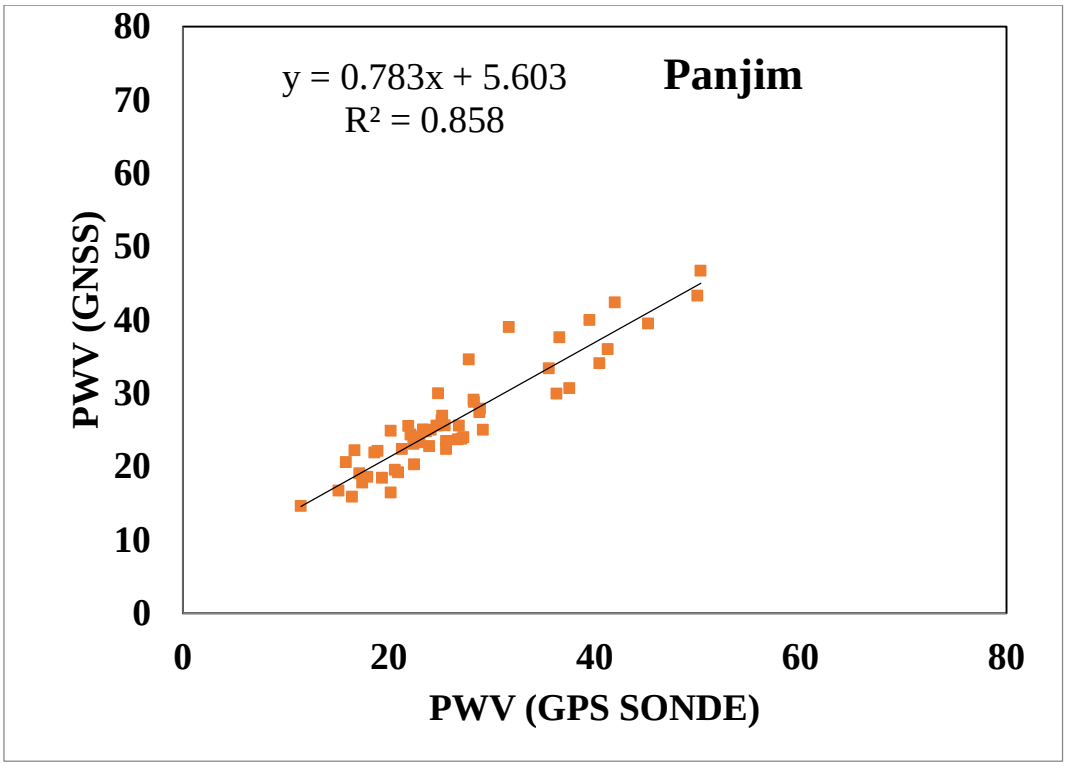

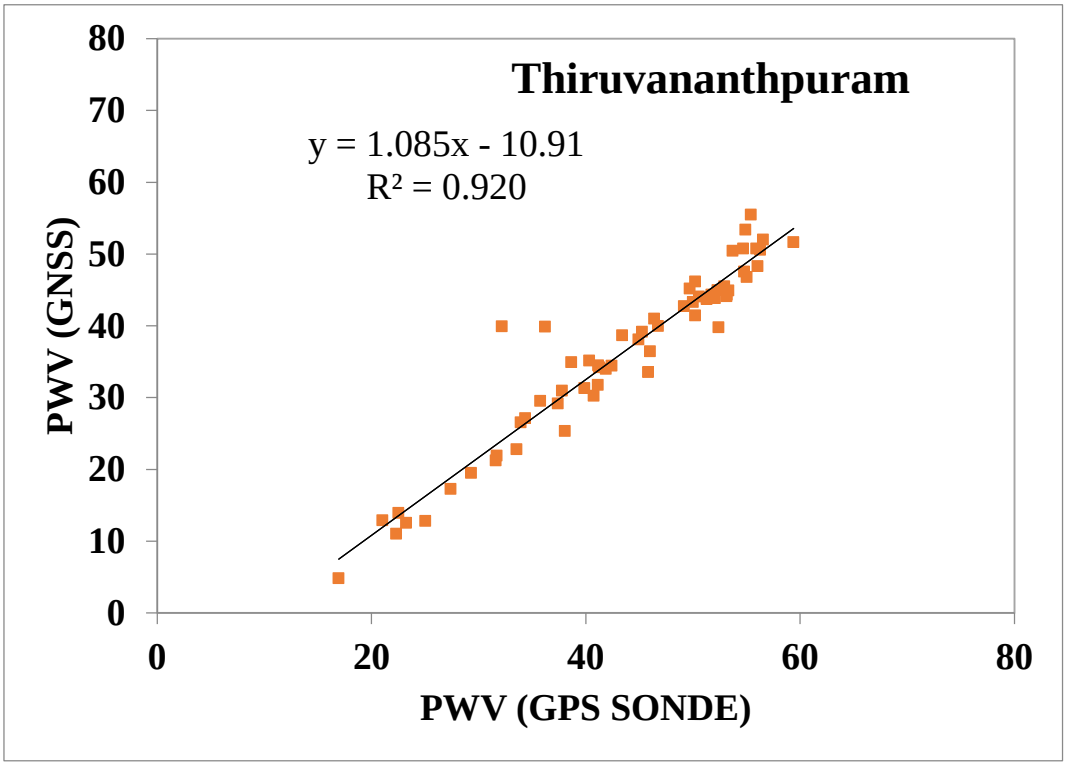

Fig. 9: Scatterplots of GNSS PWV data validated with GPS Sonde (CF06A) Yadav et. al., 2020.

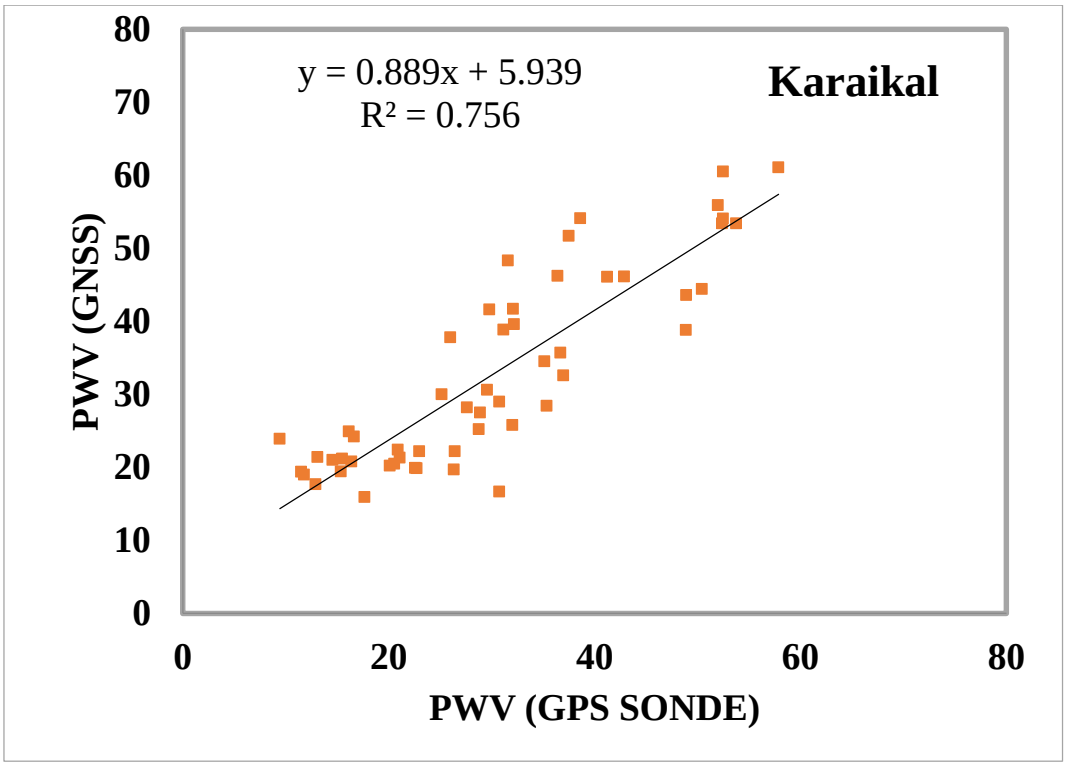
Karaikal
y = 0.889x + 5.939
R² = 0.756
PWV (GNSS)
PWV (GPS SONDE)
0
10
20
30
40
50
60
70
80
0
20
40
60
80

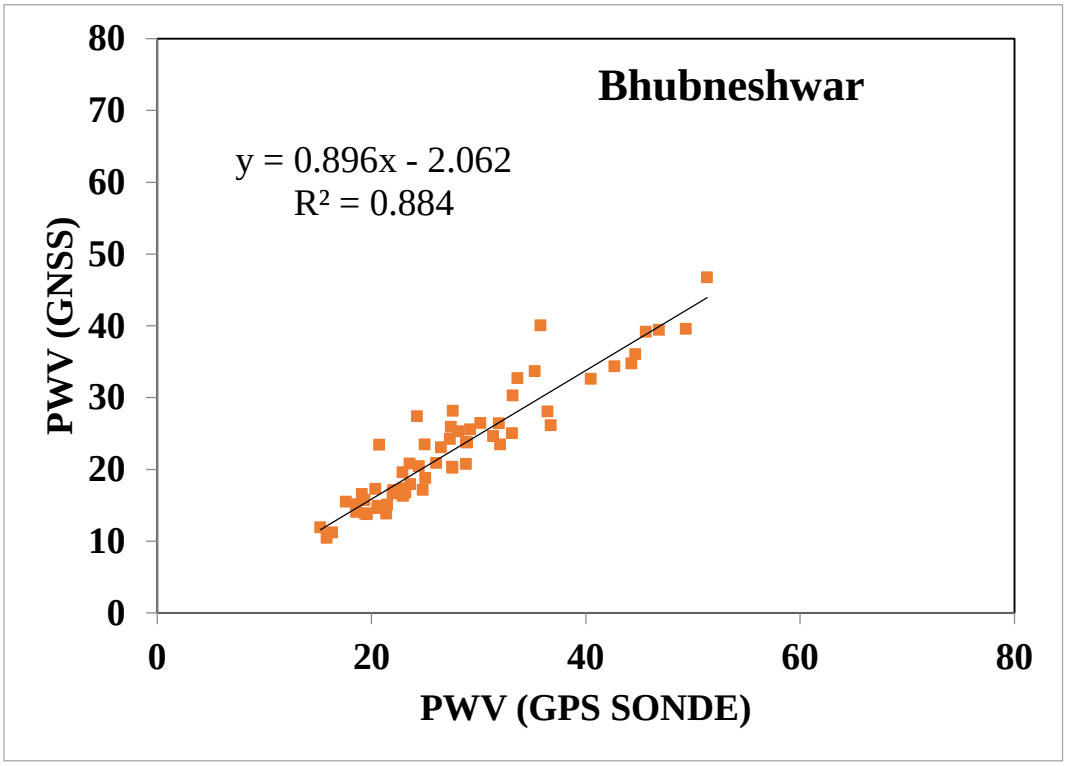
Bhubneshwar
y = 0.896x - 2.062
R² = 0.884
PWV (GNSS)
PWV (GPS SONDE)
0
10
20
30
40
50
60
70
80
0
20
40
60
80

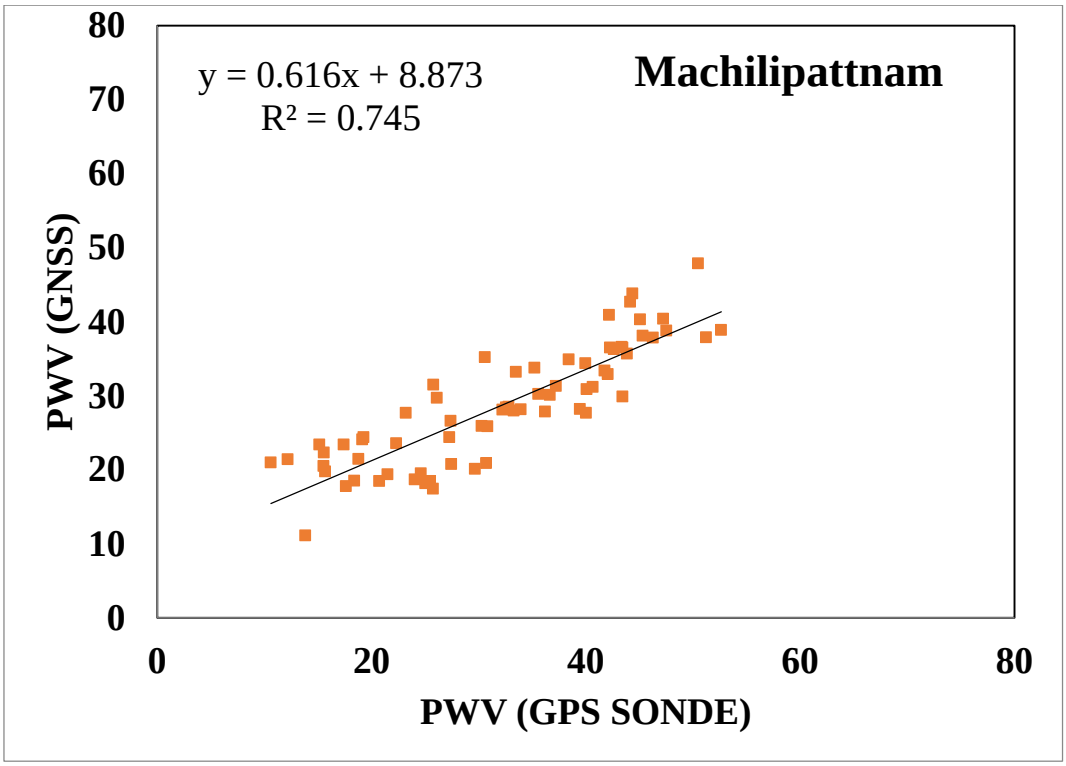

Fig. 10: Scatterplots of GNSS and GPS Sonde (RSG20A) PWV (Yadav et al., 2020).

Table 4: Validation of GNSS PWV with GPS Sonde PWV. Correlation coefficient (r), Bias and Root mean square error (RMSE) between GNSS PWV with GPS Sonde PWV are provided in the Table (Yadav et. al., 2020).

Station	r	Bias	RMSE
Delhi	0.96	-0.48	3.77
Nagpur	0.98	-0.1	1.42
Panjim	0.92	0.15	2.59
Raipur	0.85	2.50	3.67
Dibrugarh	0.90	0.80	2.35
Karaikal	0.86	-2.58	4.50
Machilipattnam	0.86	3.44	4.94
Thiruvananthpuram	0.96	7.20	5.05
Bhubneshwar	0.94	4.94	4.33

4.2 Inter-comparison of GNSS- IPWV with INSAT-3D IPWV

Space-based IPWV has inherent uncertainties and needs to be validated from time to time before using it in operational forecasting and assimilation in the NWP model. In this direction, Yadav et. al. (2020) carried out the comparison of GNSS PWV with INSAT-3D PWV for the period of June 2017 to May 2018 over the Indian region and found reasonably good agreement with INSAT-3D PWV in terms of Root Mean Square Error (RMSE), Correlation Coefficient (R), and bias of GNSS and INSAT-3D stations (Table-5). The RMSE at different stations ranged from 5.41 to 7.14 mm. The bias between GNSS and INSAT-3D sounder values of PWV was less than 1 mm except for New Delhi (1.92 mm) and Jalpaiguri (2.14 mm). Fig. 11- shows Taylor diagram for different stations which provides standard deviation, correlation coefficient, and RMS error between estimated GNSS and INSAT-3D PWV.

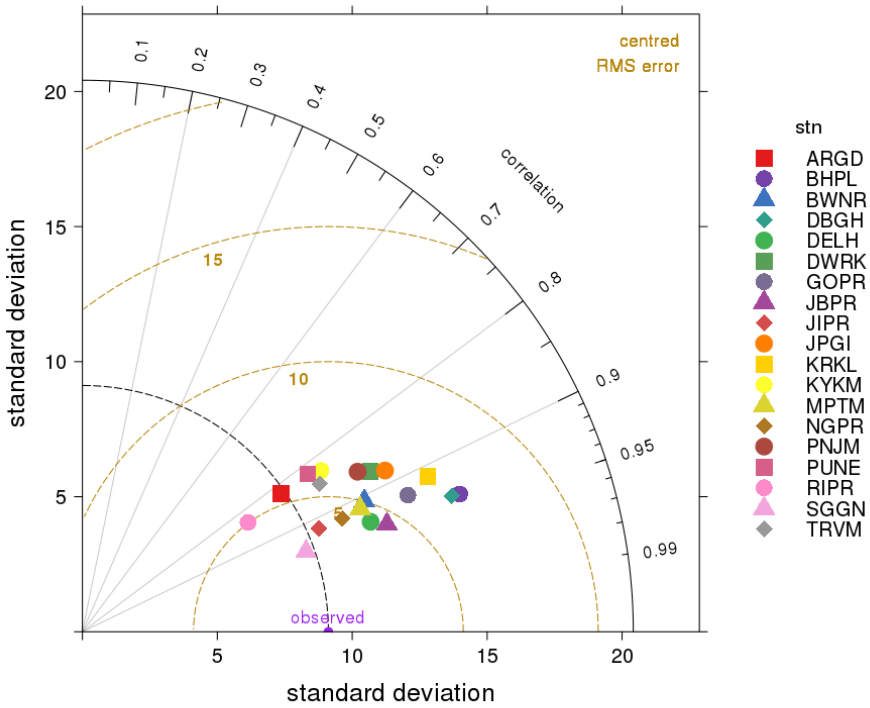

Fig. 11 Taylor diagram for GNSS PWV vs. INSAT-3D sounder derived PWV at different stations.

Table 5: Inter-comparison of GNSS- IPWV with INSAT-3D IPWV. Number of observations (N), Correlation coefficient (r), Bias and Root mean square error (RMSE) between GNSS IPWV with INSAT-3D IPWV under clear sky conditions (Yadav et. al., 2020).

Station Name	N	RMSE	r	Bias
Aurangabad	2346	5.56	0.79	0.74
Bhopal	874	5.56	0.87	-0.58
Bhubaneshwar	1357	6.40	0.88	-0.92
Dibrugarh	1069	6.44	0.92	0.39
Dwarka	2294	6.86	0.90	-4.19
Gopalpur	3332	5.91	0.87	-0.86
Jabalpur	561	6.42	0.86	-4.72
Jaipur	869	5.93	0.87	-1.38
Jalpaiguri	1541	7.14	0.87	2.14
Kanyakumari	1542	5.77	0.91	-2.59
Karaikal	1112	5.67	0.92	-1.68
Machilipattnam	1517	6.08	0.86	-3.01
Nagpur	1989	5.51	0.84	-0.51
New Delhi	1978	5.53	0.88	1.92
Panjim	1962	5.64	0.86	-0.49
Pune	478	5.96	0.86	-0.04
Shimla	808	5.51	0.81	-1.51
Thiruvananthpuram	916	5.41	0.88	0.65

4.3 Inter-comparison of GNSS- IPWV with INSAT-3DR sounder and CAMS reanalysis data

The dynamical behavior of the atmosphere in the tropics is different and hence proper validated GNSS IPWV data is required to understand better convectively driven deep circulations with fast-changing convergence and divergence areas. The comparison and validation of these data are essential so that forecasters can use these products with proper care and confidence. IPWV derived from 19 GNSS stations were intercompared with INSAT-3DR sounder retrieved data from January 2017 to June 2018 at different geographical locations over the Indian subcontinent. In this study, statistical analysis was performed in terms of root mean square error (RMSE), bias, Correlation Coefficient (CC) {Fig. 12 & 13}, and reported rmse of 8 inland stations out of 10 and 7 coastal stations out of 8 lies between 4 to 7 mm except 8 mm for Jalpaiguri (JPGI), 12 mm for Dibrugarh (DBGH) and 9 mm for Panjim stations respectively. The value of Correlation Coefficient (CC) and bias for inland stations lie in the range (0.72 to 0.93) & (-3.0 mm to +3.0 mm) respectively.

Similarly, for all the coastal stations the value of CC and bias lies in the range (0.67 to 0.88) & (-3.0 mm to +3.0 mm) respectively. Similarly, the correlation coefficient, bias, and RMSE for the desert station (SGGN) are 0.88, -1.4 mm, and 4.42 mm respectively (Fig. 12 & 13) (R. Yadav et. al., 2021). Seasonal statical analysis was also carried out by R. Yadav et. al., (2021) and reported correlation coefficient values for all the seasons between INSAT-3DR and GNSS IPWV data ranges of 0.50 to 0.98 for all the selected 19 stations except Thiruvanathpuram (0.1), Kanyakumari (0.31), Karaikal (0.15) during monsoon and Panjim (0.2) during post- monsoon season respectively.

The intercomparison review was also performed between 19 GNSS and CAMS reanalysis data from January to December 2018 at different geographical locations over the Indian subcontinent and found the RMSE differences between CAMS reanalysis & GNSS IPWV data retrievals of 9 inland stations out of 10 and 7 coastal stations out of 8 stations lie between 3 to 7 mm except 9 mm for Nagpur (NGPR) station and 14.0 mm of Bhubaneswar (BWNR) respectively. The value of Correlation Coefficient (CC) and bias for inland and coastal stations lie in the range (0.78 to 0.99 except 0.48 BWNR) & (-3.0 mm to +3.0 mm, except -6.69 mm at Pune and +7.5 mm at BWNR) respectively (Table 5). The desert station (SGGN) RMSE, CC & Bias are 3.37 mm, 0.98 and -1.74 mm respectively (Fig. 14).The RMSE values increase significantly under the wet conditions (Pre Monsoon & Monsoon season) than under dry conditions (Post Monsoon & winter season) and the differences in magnitude and sign of bias of INSAT-3DR, CAMS with respect to GNSS IPWV from station to station, and season to season.

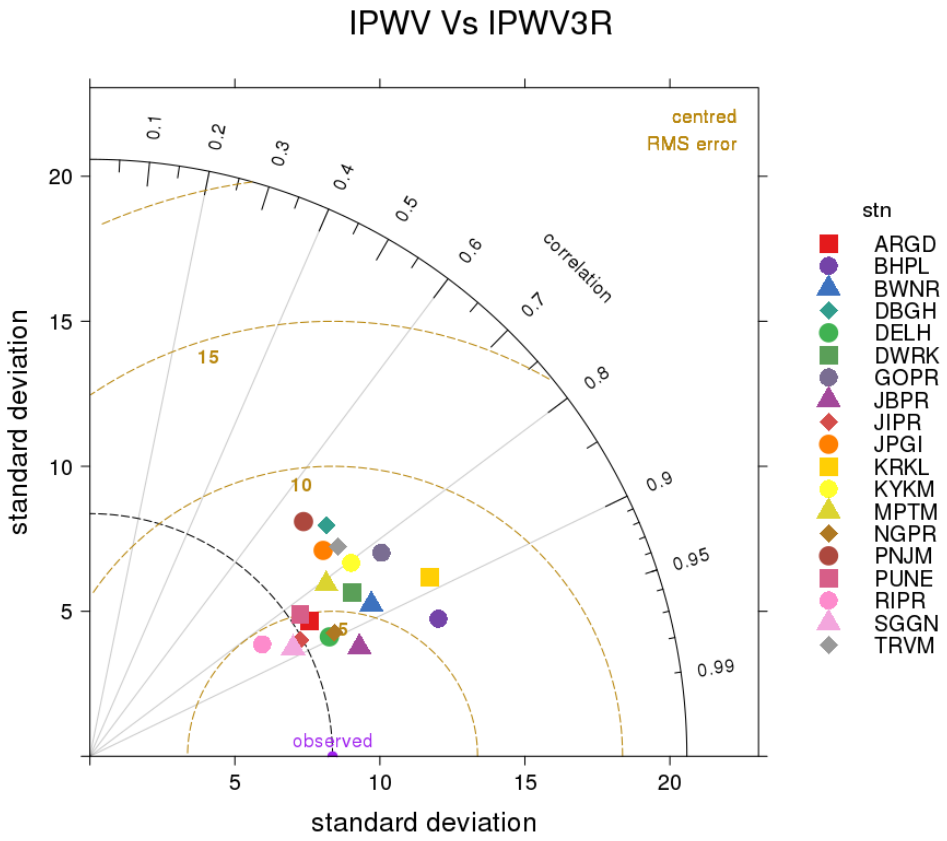

Fig. 12. Taylor diagram of INSAT-3DR vs. Indian GNSS retrievals.

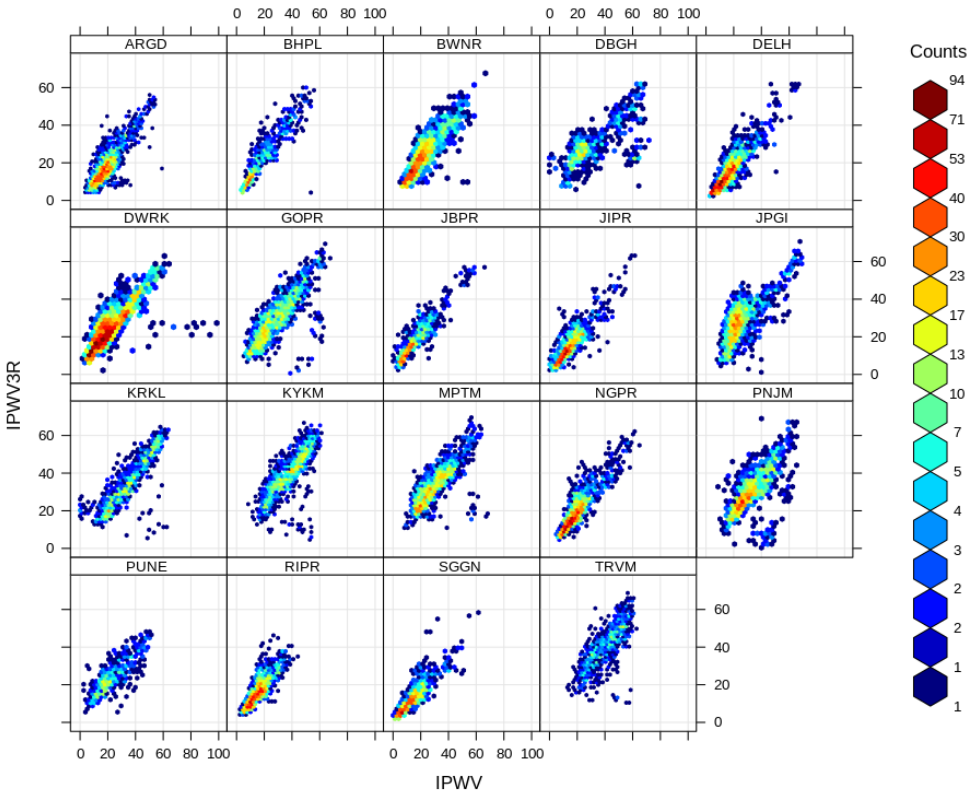

Fig. 13. Scatter plot of hourly INSAT-3DR IPWV vs. GNSS IPWV using hexagonal binning.

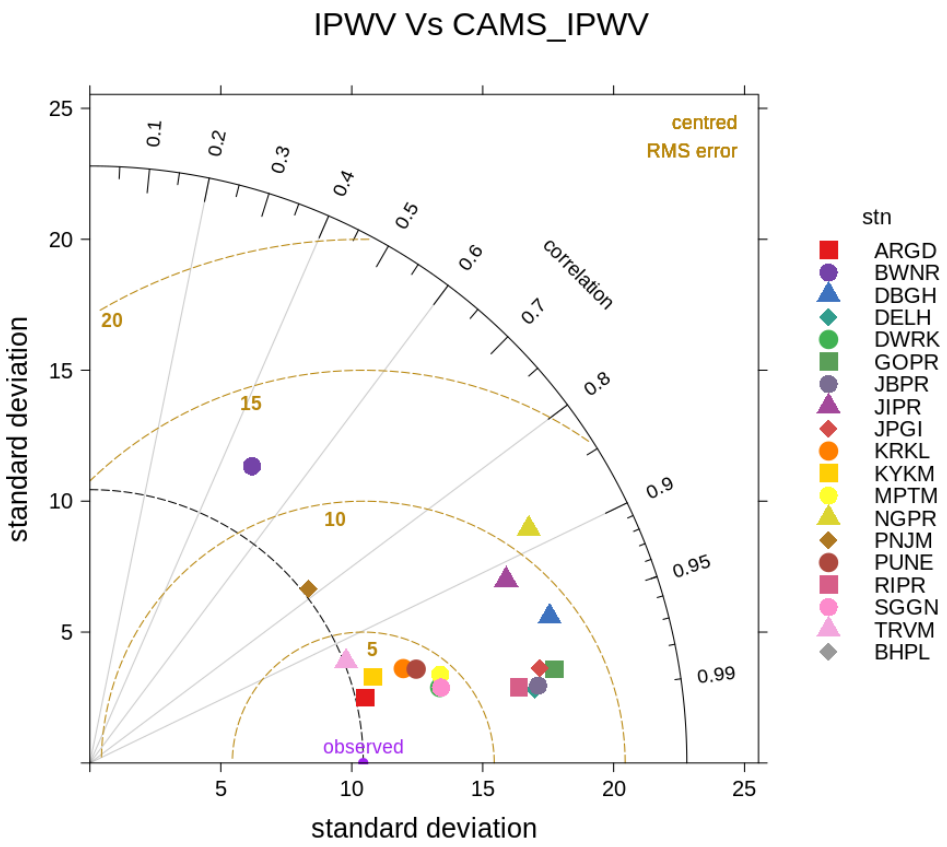

Fig. 14.Taylor diagram of CAMS vs. Indian GNSS retrievals.

Chapter-5

Month wise IPWV threshold generation for each GNSS station:

Establishing thresholds of IPWV for a location beyond which rainfall occurs could be a useful tool for the forecasts for providing rainfall forecasts over and around the location in the nowcast range. In this study, optimal sets of the thresholds for each month were determined based on the sample data of IPWV and rainfall records at the stations for each month using data for the period 2017 to 2020. A set of threshold values were determined by examining IPWV values and corresponding hourly rainfall records in each month (Fig. 15). For example for the month of June, the IPWV in the ranges of 52-58 mm were found to be associated with rainfall at Delhi. Thus, the IPWV values in this range were taken as threshold values. To further support this idea we have analysed the rate of change of IPWV (Max IPWV before rainfall – IPWV before the adjacent maximum IPWV) divided by the time interval of these two epochs (Table 6 a). It is found from the analyzed cases (Fig 15) that IPWV variation is an important and sensitive parameter to support rainfall forecasting. To incorporate the seasonal characteristics and variability of water vapour we have generated station-wise monthly thresholds of IPWV. Verification of rainfall occurrences with the month-wise thresholds of IPWV was carried out for correct and false alarm rates of Delhi for the year 2018. The overall correct rate of 86 % and false alarm rate of 14 % were found for the year 2018 (Table 6 b). The established monthly thresholds of IPWV could be useful for weather forecasting applications like nowcast prediction and monitoring the mesoscale weather events with 2-3 hours lead time (Fig 15).

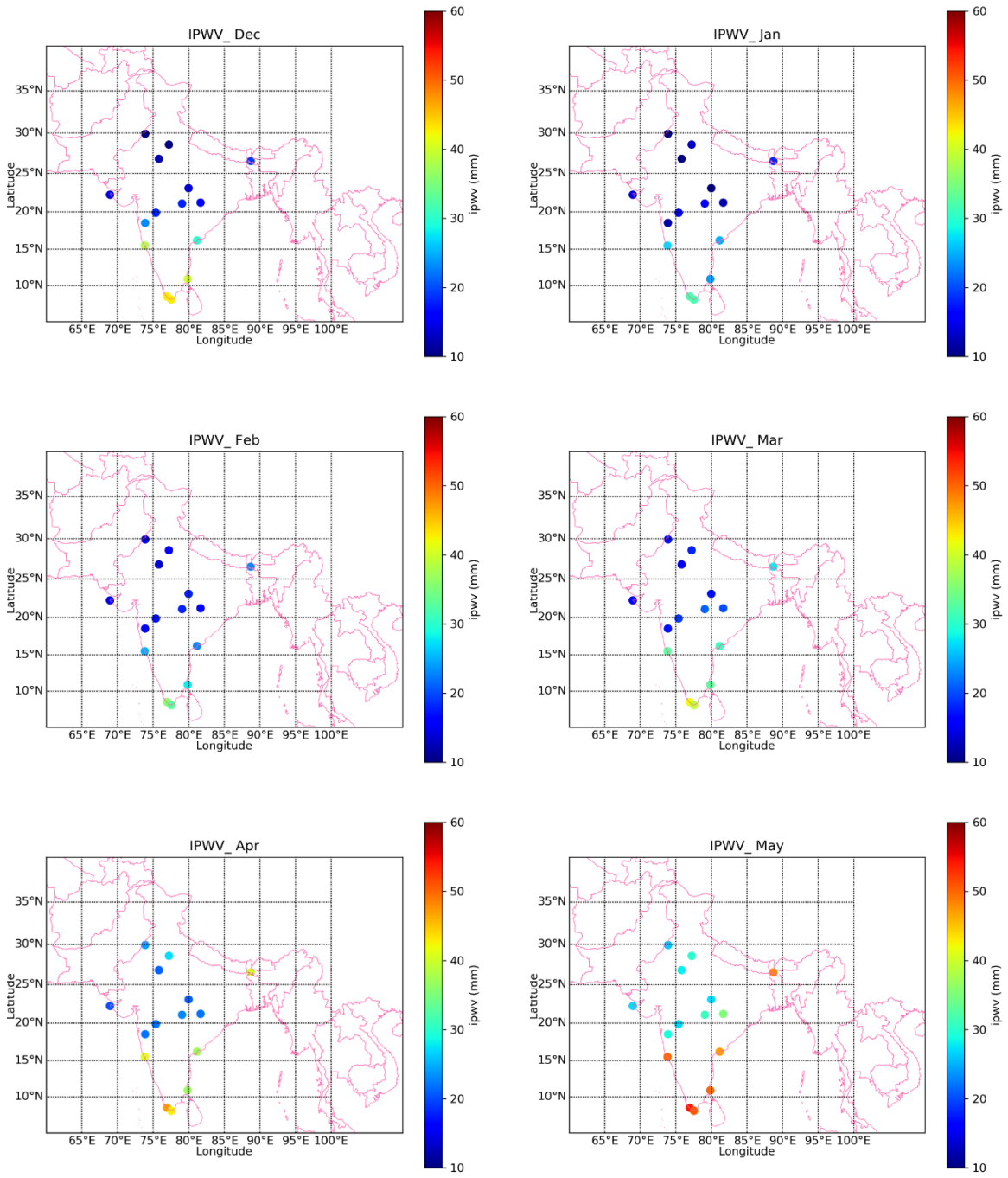
IPWV_ Dec
IPWV_ Jan
IPWV_ Feb
IPWV_ Mar
IPWV_ Apr
IPWV_ May
Latitude
Longitude
ipwv (mm)
35°N
30°N
25°N
20°N
15°N
10°N
65°E 70°E 75°E 80°E 85°E 90°E 95°E 100°E
60
50
40
30
20
10

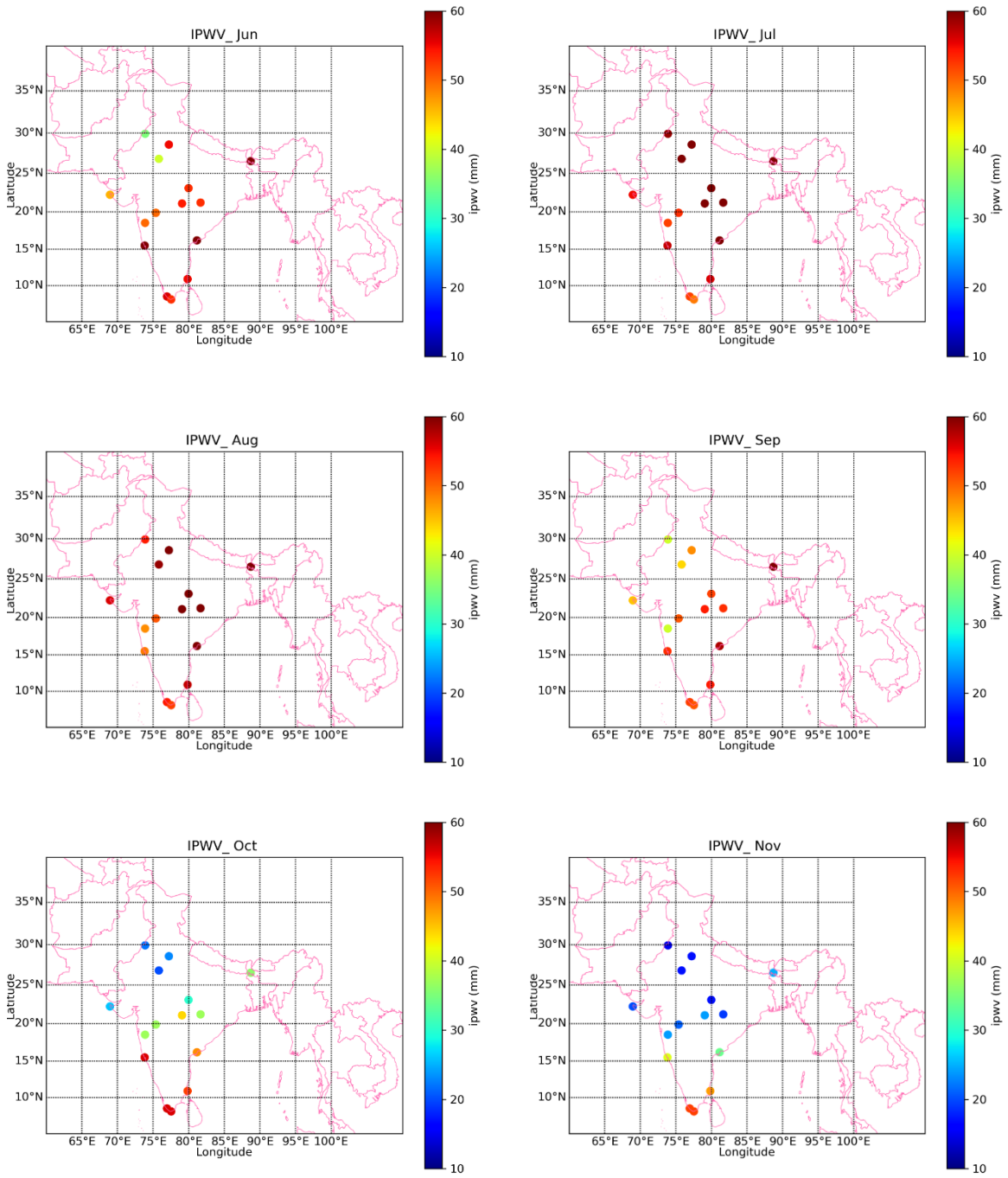

Fig. 15 spatial plot of the month-wise threshold of GNSS IPWV.

Table 6 (a) Rate of change of IPWV vs Rainfall intensity

S. No.	Stations Name Delhi	Max IPWV (mm)	Min IPWV (mm)	ΔIPWV (mm)	Interval (hr)	The rate of change of IPWV (mm/hr)	Rainfall Intensity (mm/hr)
1	Case1(April)	37	26	11	2	5.5	2.0
2	Case2 (May)	58	48	10	5	2.0	7.5
3	Case3 (June)	60	50	10	2	5.0	45.0
4	Case4 (July)	72	62	10	5	2.0	70.0

Table 6 (b) Month wise verification of thresholds with rainfall occurrence

Stations Name Delhi (2018)	Month wise IPWV threshold with rain occurrence											
	Jan	Feb	Mar	Apr	May	Jun	July	Aug	Sept	Oct	Nov	Dec
Month-wise threshold	12.61	15.39	16.63	22.85	28.92	41.86	62.82	62.37	47.01	21.40	16.80	9.66
Forecasted Frequency (no of events) Hit /Miss	2/0	--	-	8/1	5/1	2/0	16/2	19/2	7/2	-	2/1	-
Correct Rate (%)	100	--	-	90	80	100	87.5	89.5	71.5	-	67	-
False alarm rate (%)	0	--	-	10	20	0	12.5	10.5	28.5	-	33	-

Chapter-6

Preliminary Analysis of the relationship between GNSS-IPWV and Rainfall: Case studies

To examine the relationship between GNSS IPWV and rainfall, GNSS station Delhi was selected as a case study. Time-varying characteristics of IPWV during several rainfall events are shown above (Fig. 16). For this evolution, 15 minutes time interval GNSS-IPWV and hourly self-recorded rain gauge (SRRG) rainfall collocated station data used for the year 2020 on rainfall-specific dates.

It is observed from Fig. 16 that IPWV has a tendency to increase significantly before rainfall and decreases after rainfall and most of the rainfall occurs after IPWV reaches a peak. The rainfall occurred on 18th April, 30th May, 22nd June, and on 4th, 17th, 18th & 22nd July 2020. On 18th April, IPWV values fluctuated below 30 mm before the rainfall; it to increase up to its peak value of 37 mm at 13:00 UTC and 4.3 mm rainfall was recorded at 13:30 UTC. IPWV decreased to 28 mm after the rain stopped. It again increased to 31 mm at 2215 UTC and 2.9 mm rainfall was recorded at 23:00 UTC. Similarly, IPWV values reached peak values of 58 mm, 60 mm, 66.5 mm, 70.6 mm and 73 mm on 30th May, 22nd June, 4th, 17th, 18th & 22nd July 2020, and rainfall recorded was 7.5 mm on 30th May, 43.7 mm on 22nd June and 30 mm on 4th July, 8 mm on 17th July, 50 mm & 21mm (00:15 & 02:45UTC) on 18th July and 70 mm on 22nd July 2020 (Fig. 16).

Date	IPWV (mm)	Rainfall (mm/hour)
30th May	58	7.5
22nd June	60	43.5
4th July	66.5	30
17th & 18th July	70.6 67.7	8 50 & 21
22nd July	73	70

All the high IPWV values, however, did not result in occurrence of rainfall. No rainfall was recorded on 21st June 2020 inspite of a sharp increase of IPWV to about 56 mm (Fig. 16). The increase of IPWV is not the only factor to determine the occurrence of rainfall. Some external

dynamics factors such as thermodynamic variations are also necessary to trigger the rainfall. If the dynamics factors do not meet the conditions, rainfall may not occur even when the GNSS IPWV values are at a high level (Shoji et al., 2013).

Most of India is located in a monsoonal climate zone, so IPWV shows seasonal characteristics which are higher in monsoon and lower in winter. It is seen from the case study that maximum rainfall occurred while IPWV values were near to peak. IPWV analysis during the rainfall period reconfirms that the rainfall pattern is not necessary to follow the IPWV time series due to interlinked atmospheric processes. However, high spatial and temporal IPWV analysis may complement a better understanding of the tropospheric dynamics, their effects, and the future refinements in weather forecasting and numerical weather prediction regional models over the Indian region.

This study will be useful to understand the relationship of precipitation and the IPWV up to some extent and be helpful in operational forecasting by considering other parameters like combining background circulation, thermodynamic conditions, etc., especially during convective weather events. In the case four case studies for New Delhi GNSS stations, the statistical skill scores agreed reasonably well with the actual occurrence of rainfall. All the rainfall events of the year 2020 were analyzed based on the monthly threshold of IPWV and the correct rate was observed at 86 % and 14 % false alarm rate.

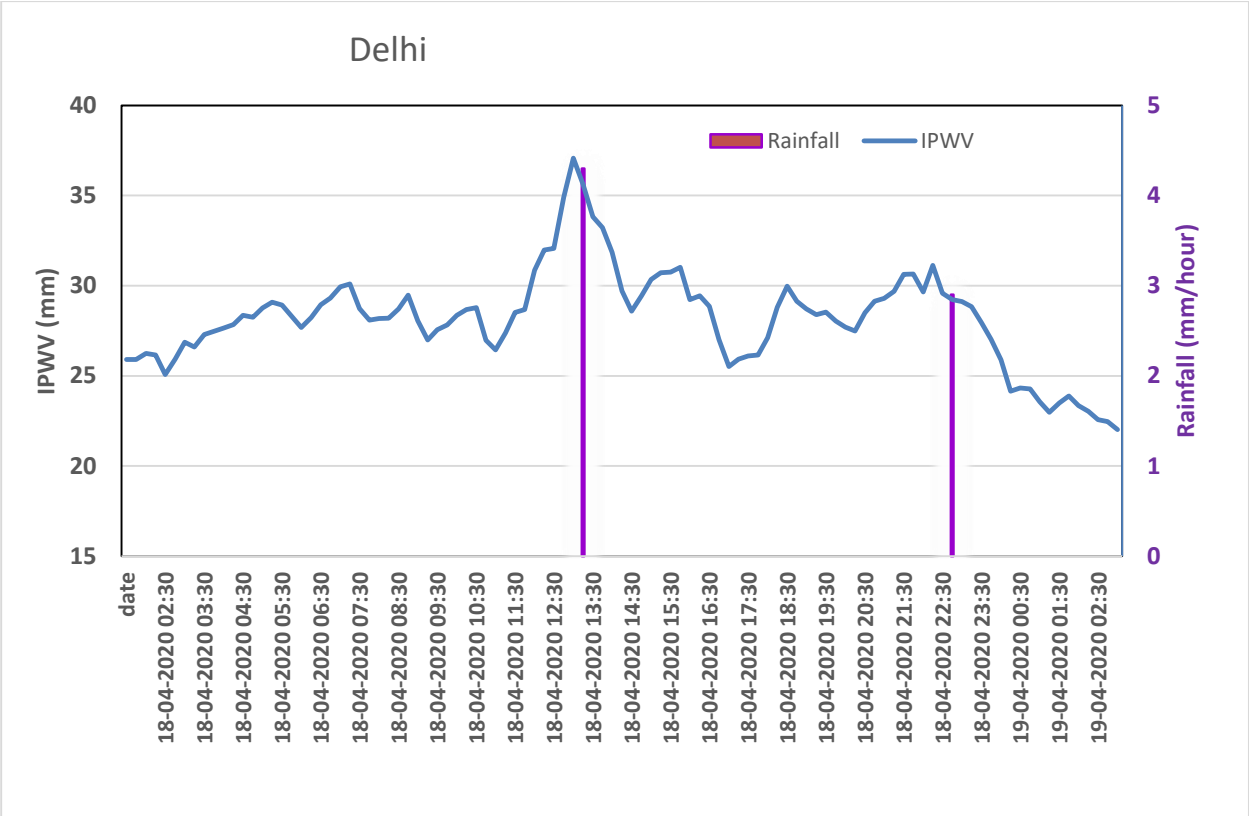
Delhi
Rainfall
IPWV
IPWV (mm)
Rainfall (mm/hour)
40
35
30
25
20
15
5
4
3
2
1
0
date
18-04-2020 02:30
18-04-2020 03:30
18-04-2020 04:30
18-04-2020 05:30
18-04-2020 06:30
18-04-2020 07:30
18-04-2020 08:30
18-04-2020 09:30
18-04-2020 10:30
18-04-2020 11:30
18-04-2020 12:30
18-04-2020 13:30
18-04-2020 14:30
18-04-2020 15:30
18-04-2020 16:30
18-04-2020 17:30
18-04-2020 18:30
18-04-2020 19:30
18-04-2020 20:30
18-04-2020 21:30
18-04-2020 22:30
18-04-2020 23:30
19-04-2020 00:30
19-04-2020 01:30
19-04-2020 02:30

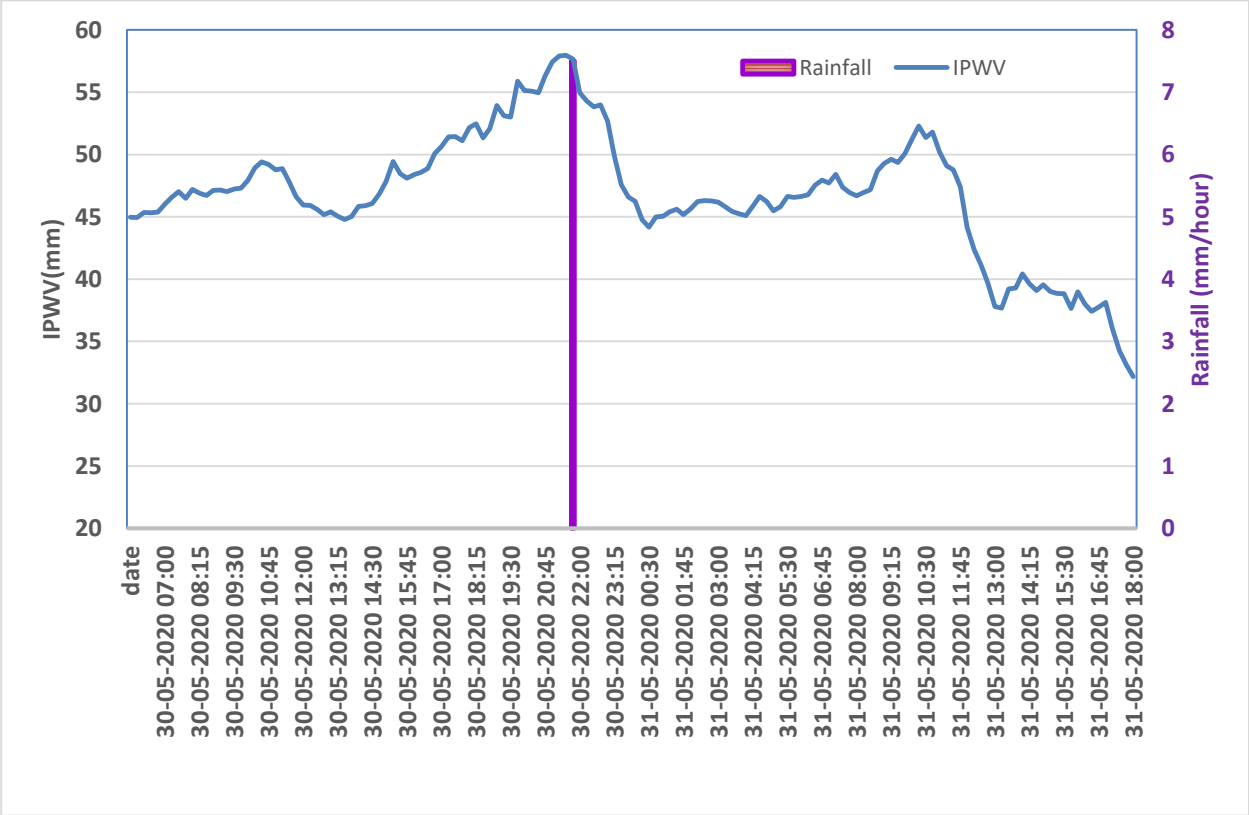
Rainfall
IPWV
IPWV(mm)
Rainfall (mm/hour)
60
55
50
45
40
35
30
25
20
8
7
6
5
4
3
2
1
0
date
30-05-2020 07:00
30-05-2020 08:15
30-05-2020 09:30
30-05-2020 10:45
30-05-2020 12:00
30-05-2020 13:15
30-05-2020 14:30
30-05-2020 15:45
30-05-2020 17:00
30-05-2020 18:15
30-05-2020 19:30
30-05-2020 20:45
30-05-2020 22:00
30-05-2020 23:15
31-05-2020 00:30
31-05-2020 01:45
31-05-2020 03:00
31-05-2020 04:15
31-05-2020 05:30
31-05-2020 06:45
31-05-2020 08:00
31-05-2020 09:15
31-05-2020 10:30
31-05-2020 11:45
31-05-2020 13:00
31-05-2020 14:15
31-05-2020 15:30
31-05-2020 16:45
31-05-2020 18:00

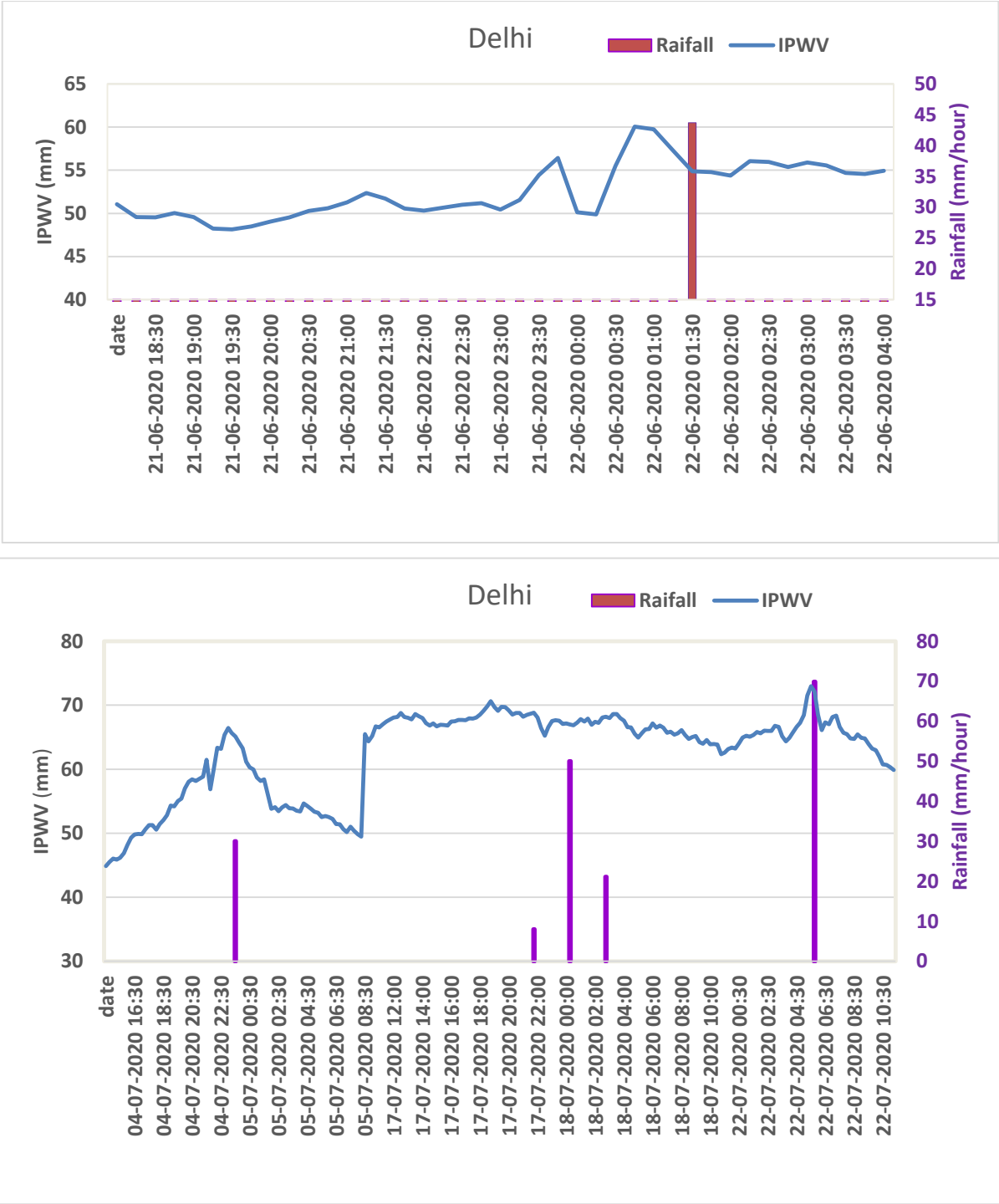

Fig. 16 the relationship between GNSS-IPWV and several rainfall events at station Delhi. Blue line represents IPWV and voilet line represents hourly rainfall.

Acknowledgements

The authors are grateful to the Director-General of Meteorology of the India Meteorological Department for all-time the support and guidance during the study. The support of other colleagues of the satellite meteorology division of IMD to further refine the work is highly appreciated.

References:

- Aumann, H. H., Chahine, M. T., Gautier, C., Goldberg, M. D., Kalnay, E., McMillin, L. M., and Revercomb, H.: AIRS/AMSU/HSB on the Aqua mission: Design, science objectives, data products, and processing systems, IEEE Trans. Geosci. Remote Sens., 41, 253–264, 2003.
- Beirle, S., Lampel, J., Wang, Y., Mies, K., Dörner, S., Grossi, M., Loyola, D., Dehn, A., Danielczok, A., Schröder, M., and Wagner, T.: The ESA GOME-Evolution "Climate" water vapor product: a homogenized time series of H2O columns from GOME, SCIAMACHY, and GOME-2, Earth Syst. Sci. Data, 10, 449–468, https://doi.org/10.5194/essd-10-449-2018, 2018.
- Berrisford, p., Kallberg, P., Kobayashi, S., Dee, D., Uppala S., Simmons, A. J., Poli, P., and Sato, H.: Atmospheric conservation properties in ERA-Interim, Q. J. R. Meterol. Soc., 137, 1381–1399, 2011.
- Bevis, M., S. Businger, T. A. Herring, C. Rocken, R. A. Anthes, and R. Ware (1992), GPS Meteorology: Remote sensing of atmospheric water vapor using the Global Positioning System, J. Geophys. Res., 97(D14), 15,787–15,801.
- Bevis, M., S. Businger, and S. Chiswell (1994), GPS meteorology: Mapping zenith wet delays on to Precipitable water, J. Appl. Meteorol., 33,379–386.
- Bouma, H.R., (2002) Lic. Thesis. Tech. Rep. L. Ground-based GPS in Climate Research, vol. 456 School of Electrical and Computer Engineering, Chalmers University of Technology, Sweden.

  Davis, J.P., and R. Smalley Jr. 2009. Love wave dispersion in central North America determined using absolute displacement seismograms from high-rate GPS. Journal of Geophysical Research 114: B11303. doi:10.1029/2009JB006288.
- Chen, B., Z. Liu., (2016) Global water vapor variability and trend from the latest 36 year (1979 to 2014) data of ECMWF and NCEP reanalyses, radiosonde, GPS, and microwave satellite, J. Geophys.Res. Atmos., 121, 11,442–11,462, doi: 10.1002/2016JD024917.
- Dai, A., (2001) Global precipitation and thunderstorm frequencies, II, Diurnal variations. J. Clim. 4, 1112–1128.
- Emmanuel, M., Sunilkumar, S.V., Ratnam, M.V., Muhsin, M., Parameswaran, K., Murthy, B.V.K., (2018) Diurnal variation of the tropospheric water vapour a coastal and an inland station in Souther India peninsula. J. Atmosp. Solar-Terrest. Phys. 179, 11–21. https://doi.org/10.1016/j.jastp.2018.06.007.

- Gelaro, R., McCarty, W., Suarez, M. J., Todling, R., Molod, A., Takacs, L., Randles, C. A., Darmenov, A., Bosilovich, M. G., Reichle, R., Wargan, K., Coy, L., Cullather, R., Draper, C., Akella, S., Buchard, V., Conaty, A., Da Silva, A. M., Gu, W., Kim, G.-K., Koster, R., Lucchesi, R., Merkova, D., Nielsen, J. E., Partyka, G., Pawson, S., Putman, W., Rienecker, M., Schubert, S. D., Sienkiewicz, M., and Zhao, B.: The Modern-Era Retrospective Analysis for Research and applications, Version 2 (MERRA-2), J. Climate, 30, 5419–5454, 2017.
- Güldner, J., Spänkuch, D., (1999) Results of year-round remotely sensed integrated water vapor by ground-based microwave radiometry. J. Appl. Meteorol. 38, 981–988.
- Haldar, G.C., Sud, A.M., Marathe, S; D., (1991) Diurnal variation of monsoon rainfall in central India. Mausam 42: 37–40.
- Hagemann, S., L. Bengtsson, and G. Gendt (2003), On the determination of atmospheric water vapor from GPS measurements, J. Geophys. Res., 108(D21), 4678, doi:10.1029/2002JD003235.
- Jiang, J., Zhou, T., and Zhang, W.: Evaluation of satellite and reanalysis precipitable water vapor data sets against radiosonde observations in central Asia, Earth and Space Science, 6, 1129–1148, https://doi.org/10.1029/2019EA000654, 2019.
- Kaufman, Y. J. and Gao, B.-C.: Remote sensing of water vapor in the near IR from EOS/MODIS, IEEE T. Geosci. Remote, 30, 871–884, 1992.
- Kishtawal, C. M.: Use of satellite observations for weather prediction, Mausam, 70, 709–724, 2019.
- Kimura, F., Tanikawa, R., Yoshizaki, M., (1997) Diurnal variation of precipitable water in clear days over the northern mountains in Kanto plain. Tenki 44, 799–807 in Japanese.
- Kuwagata, T., Numaguti, A., Endo, N., (2001) Diurnal variation of water vapor over the Central Tibetan Plateau during summer. J. Meteorol. Soc. Jpn. 79 (1B), 401–418.
- Koteswaram, FNA, P., (1978): Meteorology and climatology of the Rajasthan Desert. Proc. Indian natn. Sci. Acad. Vol.44, Part B, No.6, pp. 401-410.
- Koulali, A., Ouazar, D., Bock, O., Fadil, A., (2012) Study of seasonal-scale atmospheric water cycle with ground based GPS receivers, radiosondes, and NWP models over Morocco. Atmos. Res. 104-105, 273-291.
- Liu, X., Bai, A., Liu C., (2009) Diurnal variations of summer time precipitation over the Tibetan plateau in relation to orographically induced regional circulations. Environmental Research Letters. DOI: 10.1088/1748-9326/4/4/045203.

- Mendis, V. B., Prates, G., Santoa, L., Langley, R. B., 2000. An evaluation of the accuracy of models for the determination of the weighted mean temperature of the atmosphere. Proceeedings of ION 2000, National Technical Meeting, Anaheim, CA, USA, pp. 433-438. (xref).
- Miloshevich, L. M., Vömel, H., Whiteman, D. N., and Leblanc, T.: Accuracy assessment and correction of Vaisala RS92 radiosonde water vapor measurements, J. Geophys. Res., 114, D11305, https://doi.org/10.1029/2008JD011565, 2009.
- Mieruch, S., Noel, S., Noel, S., Bovensmann, H., Burrows, J. P., (2008) Analysis of global water vapour trends from satellite measurements in the visible spectral range. Atmospheric Chemistry and Physics, 8(3), 491–504.
- Murakami, M., (1983) Analysis of the deep convective activity over the western Pacific and Southeast Asia. J. Meteor. Soc. Japan 61, 60–75.
- Niell, A. E., (1996). "Global mapping functions for the atmosphere delay at radio wavelengths", J. Geophys. Res. 101(B2):3227-3246.
- Nitta, T., Sekine, S., (1994) Diurnal variation of convective activity over the tropical western Pacific. J. Meteor. Soc. Japan 72, 627–641.
- Ohsawa, T., Ueda, H., Hayashi, T., Watanabe, A., Matsumoto, J., (2001) Diurnal variations of convective activity and rainfall in tropical Asia. J. Meteor. Soc. Japan 79, 333–352.
- Oki, T., Musiake, K., (1994) Seasonal change of the diurnal cycle of precipitation overJapan and Malaysia. J. Appl. Meteorol. 33, 1445–1463.
- Ohtani, R., (2001) Detection of water vapor variations driven by thermally induced local circulations using the Japanese continuous GPS array. Geophys. Res. Lett. 28, 151–154.
- Ortiz de Galisteo, J.P., Cachorro,V., Toledano, C., Torres, B., Laulainen, N., Bennouna, Y., de Frutos,A., (2011) Diurnal cycle of precipitable water vapor over Spain. Q J Roy Meteor Soc. 137(657):948–958. https://doi.org/10.1002/qj.811.
- Puviarasan, N., Sharma, A. K., Ranalkar, M., & Giri, R. K. (2015). Onset, advance and withdrawal of southwest monsoon over Indian subcontinent: A study from precipitable water measurement using ground based GPS receivers. Journal of Atmospheric and Solar-Terrestrial Physics, 122, 45–57.
- Puviarasan, N., Yadav, R., Giri, R. K., and Singh, V.: GPS Meteorology: Error in the estimation of precipitable water by ground based GPS system in some meso-scale thunderstorms – A case study, Mausam, 71, 175–186, 2020.

- Parracho, Ana C., Bock, Olivier.,Bastin, Sophie., (2018) Global IWV trends and variability in atmospheric reanalyses and GPS observations, Atmos. Chem. Phys., 18, 16213–16237.
- Pramualsakdikul, S., Haas, R., Elgered, G., Scherneck, H.G., (2007) Sensing of diurnal and semi-diurnal variability in the water vapour content in the tropics using GPS measurements. Meteorol. Appl. 14, 403–412
- Rakhecha, Pukhraj. (2018). Hydrometeorology of the Rajasthan desert rainfall. International Journal of Hydrology. 2. 10.15406/ijh.2018.02.00144.
- Rohm, W., Yuan, Y., Biadeglgne, B., Zhang, K., Le Marshall, J., (2014) Ground-based GNSS ZTD/IWV estimation system for numerical weather prediction in challenging weather conditions. Atmos. Res. 138, 414-426.
- Saha, S.: The NCEP climate forecast system reanalysis, Bull. Am. Meteorol. Soc., 91, 1015–1057, 2010.
- Shoji, Y. Retrieval of water vapor inhomogeneity using the Japanese nationwide GNSS array and its potential for prediction of convective precipitation. Journal of the Meteorological Society of Japan. 91, 43–62 (2013).
- Schueler, T., Posfay, A., Hein, G.W., Biberger, R., 2001. A global analysis of the mean atmospheric temperature for GPS water vapor estimation. C5: atmospheric effects, IONGPS2001 – 14th International Technical Meeting of Satellite Division of the Institute of Navigation, Salt Lake City, Utah. (xref).
- Solbrig, P., 2000. Untersuchungen uber die Nutzung numerischer Wettermodelle zur Wasserdampfbestimmung mit Hilfe des Global Positioning Systems. Diploma Thesis, Insitute of Geodesy and Navigation, University FAF Munich, Germany. (xref).
- Stevens, B., Brogniez, H., Kiemle, C., Lacour, J.-L., Crevoisier, C., Kiliani, J., (2017) Structure and dynamical influence of water vapor in the lower tropical troposphere. Surv. Geophys. 38, 1371–1397. https://doi.org/10.1007/s10712-017-9420-8.
- Trenberth, K.E., Dai, A., Rasmussen, R.M. and Parsons, D.B. (2003) The changing character of precipitation. Bulletin of the American Meteorological Society, 84, 1205–1217. https://doi.org/10.1175/BAMS-84-9-1205.
- Turner, D. D., Lesht, B. M., Clough, S. A., Liljegren, J. C., Revercomb, H. E., and Tobin, D. C.: Dry bias and variability in Vaisala RS80-H radiosondes: The ARM experience, J. Atmos. Ocean. Tech., 20, 117–132, 2003.
- Wang, J. H., Zhang, L. Y., Dai, A. G. 2005: Global estimates of water-vapor-weighted mean temperature of the atmosphere for gps applications. J. Geophys. Res., 110(D21101).

- Wang, J., Zhang, L., Dai, A., Van Hove, T., Van Baelen, J., (2007) A nearglobal,2-hourly data set of atmospheric precipitable water from ground-based GPSmeasurements. J. Geophys. Res. 112:D11107, DOI: 10.1029/2006JD007529.
- Wu, P., Hamada, J.-I., Mori, S., Tauhid, Y.I., Yamanaka, M.D., (2003) Diurnal variation of precipitable water over mountainous area of Sumatra Island. J. Appl. Meteor. 42, 1107–1115. https://doi.org/10.1175/1520-0450.
- Yadav, R., Puviarasan, N., Giri, R. K., Tomar, C. S., and Singh, V.: Comparison of GNSS and INSAT-3D sounder retrieved precipitable water vapour and validation with the GPS Sonde data over Indian Subcontinent, MAUSAM, 71, 1–10, available at: https://mausamjournal.imd.gov.in/index.php/MAUSAM/article/view/1, last access: 20 May 2020.
- Yadav, R., Giri, R. K., and Singh, V.: Intercomparison review of IPWV retrieved from INSAT-3DR sounder, GNSS and CAMS reanalysis data, Atmos. Meas. Tech., 14, 4857–4877, https://doi.org/10.5194/amt-14-4857-2021, 2021.